



HAL
open science

Spatial patterning of Middle Palaeolithic lithic assemblages at the Abri du Maras, Southeast France: combining GIS analysis and 3D palaeotopographic reconstructions

Pierre Guillemot, Stéphane Jaillet, M Gema Chacón, Véronique Pois, Marie-Hélène Moncel

► To cite this version:

Pierre Guillemot, Stéphane Jaillet, M Gema Chacón, Véronique Pois, Marie-Hélène Moncel. Spatial patterning of Middle Palaeolithic lithic assemblages at the Abri du Maras, Southeast France: combining GIS analysis and 3D palaeotopographic reconstructions. *Journal of Archaeological Science: Reports*, 2023, 49, pp.103999. 10.1016/j.jasrep.2023.103999 . hal-04070818

HAL Id: hal-04070818

<https://hal.science/hal-04070818>

Submitted on 16 Apr 2023

HAL is a multi-disciplinary open access archive for the deposit and dissemination of scientific research documents, whether they are published or not. The documents may come from teaching and research institutions in France or abroad, or from public or private research centers.

L'archive ouverte pluridisciplinaire **HAL**, est destinée au dépôt et à la diffusion de documents scientifiques de niveau recherche, publiés ou non, émanant des établissements d'enseignement et de recherche français ou étrangers, des laboratoires publics ou privés.



Distributed under a Creative Commons Attribution - NonCommercial - NoDerivatives 4.0 International License

1 **Authors:**

2
3 Pierre GUILLEMOT^{a*}, Stéphane JAILLET^b, M. Gema CHACÓN^{c,d,a}, Véronique POIS^e
4 Marie-Hélène MONCEL^a

5
6 ^a UMR 7194, CNRS, Département Homme & Environnement, Muséum National d'Histoire Naturelle, UPVD,
7 Sorbonne Universités, 1 René Panhard, 75013, Paris, France (* Corresponding author: p.guillemot@icloud.com)

8 ^b Laboratoire Environnement Dynamiques et Territoires de Montagne (EDYTEM), UMR 5204, 73376 Le
9 Bourget du Lac, France.

10 ^c Institut Català de Paleoecologia Humana i Evolució Social (IPHES – CERCA), Zona Educativa 4, Campus
11 Sescelades URV (Edifici W3), Tarragona 43007, Spain

12 ^d Departament d'Història i Història de l'Art, Universitat Rovira i Virgili (URV), Av. Catalunya 35, 43002
13 Tarragona, Spain

14 ^e Université de Perpignan Via Domitia (UPVD), UMR 7194 CNRS, MNHN– HNHP, Centre Européen de
15 Recherches Préhistoriques de Tautavel, 66720 Tautavel, France

16
17 **Title:**

18
19 **Spatial patterning of Middle Palaeolithic lithic assemblages at the Abri du**
20 **Maras, Southeast France: combining GIS analysis and 3D**
21 **palaeotopographic reconstructions**

22
23
24 **Abstract:**

25
26 The intra-site spatial analysis of prehistoric assemblages is a topical way of assessing the use
27 of space by ancient hominins. Such approaches can bring to light how prehistoric groups
28 occupied their living space and organised activity areas, and thus describe their cultural and
29 social behaviours. The Abri du Maras in Southeast France is a major Middle Palaeolithic site
30 with huge potential for characterising the cognitive and technological behaviours of
31 Neanderthals. In this study, we carry out a high-resolution spatial analysis focusing primarily
32 on the lithic assemblages of levels 4.1 and 4.2, dated to MIS 3. The methodology combines
33 two approaches: the use of GIS tools selected from free and open-source QGIS software, and
34 palaeosurface rendering, using 3D software, in order to incorporate palaeotopographic data
35 into the spatial analysis. Data for these palimpsests show a structured spatial patterning of
36 occupations with some differences between the two levels. In level 4.1, a clear spatial pattern
37 is observed with main areas where intense knapping activities were carried out and peripheral
38 areas where specific remains were located. The spatial pattern for level 4.2 appears less clear,
39 but also revealed patterns related to the type of remains. Our analysis provides evidence of
40 complex spatial organisation for Neanderthals and corroborates previous results from other
41 Middle Palaeolithic sites. We also highlight the relevance of our methodology, combining
42 free and open-source GIS tools and palaeotopographic rendering, as well as the
43 complementarity of 2D-3D tools, to achieve high-resolution spatial analysis of Palaeolithic
44 sites.

45
46 **Keywords:** Spatial pattern, GIS analysis, Lithic assemblages, 3D palaeotopographic
47 rendering, Middle Palaeolithic, Abri du Maras

51 1. Introduction

52

53 Spatial analysis is an effective tool for assessing the relationship between
54 archaeological material and hominin behaviours and revealing small- and large-scale spatial
55 patterns. It consists of two main approaches: inter-site analysis and intra-site analysis (Coil,
56 2016). Intra-site spatial analysis focuses on the material in individual sites through the study
57 of site formation processes (taphonomy) and spatial patterning in order to assess social,
58 economic or symbolic behaviours. In modern society, specific activities are related to
59 particular areas (Alperson-Afil and Hovers, 2005; Anderson and Burke, 2008). Therefore, one
60 of the assumptions underlying intra-site spatial analysis in archaeology is that similar
61 associations can be observed in the archaeological record. Thus, spatial analysis has been an
62 essential tool for many decades now, allowing archaeologists to better understand the
63 behaviour of early hominins through the way they used space.

64 Due to their apparent lack of complexity, Middle Palaeolithic spatial structures have
65 long been debated. Initially, some authors described Neanderthal spatial patterning as less
66 complex than that of modern humans, comparing it to carnivores, such as hyenas (Pettitt,
67 1997), or as a simple and instinctive response to the environment (Mellars, 1996). However,
68 these ideas have been criticised and some Lower and Middle Palaeolithic spatial structures
69 have been considered as “modern” and similar to those described for *Homo sapiens*
70 (Alperson-Afil, 2008; Alperson-Afil et al., 2009; Alperson-Afil and Hovers, 2005; Henry,
71 2012; Henry et al., 2004; Neruda, 2017; Oron and Goren-Inbar, 2014; Vaquero et al., 2001;
72 Vaquero and Pastó, 2001).

73 The question of Neanderthal modernity was recently raised at the Abri du Maras. This
74 rock shelter has yielded the oldest evidence of cord making known to date (Hardy et al.,
75 2020). This fibre technology requires a complex knowledge of plants and the understanding
76 of mathematical concepts for creating and managing pairs of numbers to create a string
77 structure. Consequently, the authors consider Neanderthals as the cognitive equals of modern
78 humans (Hardy et al., 2020). Therefore, the potential of the Abri du Maras for characterising
79 the behaviour and technological capacities of Neanderthal has already been proven (Hardy et
80 al., 2020, 2013; Moncel et al., 2021, 2014). In this context, this paper presents a high-
81 resolution spatial analysis, focusing primarily on the comparison of the lithic assemblages of
82 levels 4.1 and 4.2, dated to MIS3 (Richard et al., 2021, 2015), and considered as short-term
83 occupations by the technological and subsistence strategies (Moncel et al., 2021, 2014). We
84 combine innovative GIS (Geographic Information System) tools and palaeosurface rendering
85 using 3D software. The main objective is to examine the occupation patterns of human groups
86 at the Abri du Maras in relation to the topographical contexts of the site (Guillemot 2021).
87 Through the study of two archaeological levels, we analyse and compare how occupants
88 structured their inhabited space in a limited period of time.

89

90 2. The dataset

91 2.1. Chronological and archaeological context of the Abri du Maras

92

93 The Abri du Maras is a vast rock shelter located in a small valley near the Ardèche
94 River, downstream of the Ardèche gorges. It is currently 12 m long, and 3 m deep with a
95 ceiling height of 2 m (Combiér, 1967). The first excavations in the 1950s-1960s by R. Gilles
96 and J. Combiér unearthed a stratigraphic sequence of eight archaeological layers with Middle
97 Palaeolithic deposits and a Levallois laminar debitage at the top of the sequence (Moncel et
98 al., 1994). Those layers record the gradual collapse of the cave roof over time (Debard, 1988).

99 New excavations in front of the shelter since 2006 have focused on the middle and lower part
100 of the stratigraphic sequence, only intermittently excavated during former fieldwork.

101 The new sequence records six stratigraphic units. Stratigraphic layer 6 is currently the
102 oldest known unit bearing evidence of human presence (Moncel et al., 2018) and lies directly
103 on the limestone substratum (Moncel et al., 2021). Layer 5 is made up of an organic brown
104 unit with a sandy-silty matrix (Moncel et al., 2014). Three occupation phases have been
105 identified in this layer and dated to the end of MIS 5 (Marín et al., 2020; Richard et al., 2015).
106 The overlying upper deposit is layer 4, 0.5 to 1 m thick, consisting of blocks of various sizes
107 in loessic lenses. This coarse infilling contains two phases of occupation (levels 4.1 and 4.2)
108 separated by a sterile loessic layer, dated to MIS 3 (level 4.1: between 40 ± 3 ka and 46 ± 3 ka
109 ; level 4.2: between 42 ± 3 ka and 55 ± 2 ka) (Richard et al., 2015). More recent
110 chronological data confirm these ages and the attribution of the sequence to MIS 3 (Richard et
111 al., 2021). Layer 4 was deposited during progressively colder and drier conditions (Puaud et
112 al., 2015) and the faunal corpus is composed in order of abundance of *Rangifer tarandus*,
113 *Equus ferus* cf. *germanicus*, *Cervus elaphus*, *Bison priscus*, *Capra ibex*, *Equus hydruntinus*
114 and *Megaloceros giganteus* (Daujeard et al., 2019). While the reindeer largely dominates the
115 level 4.1 faunal assemblage, level 4.2 does not show such a mono-specific spectrum. Core
116 technology consists of diverse, often short debitage sequences, including Levallois type
117 debitage, made on local flint collected within 15-30 km of the site. The lithic assemblage and
118 refits attest to short-term occupations with mostly unretouched flint flakes, blades, bladelets
119 and points. Large ready-to-use flakes, blades and points were also brought to the shelter while
120 additional *in situ* debitage produced small flakes (Moncel et al., 2021, 2014). The two layers
121 have been considered as evidence of repeated short-term occupations.

122 The new excavations extend over a surface of around 50 m² for levels 4.1 and 4.2,
123 which only represents part of the available surface of the shelter during human occupations.
124 The accumulation and position of blocks from the collapse of the shelter indicate possibly the
125 limits of the shelter ceiling during the occupation of levels 4.1 and 4.2. The ceiling border was
126 estimated to be located in bands 8/9.

127 Excavations were conducted using a square metre grid. Each object, larger than 2 cm
128 for faunal remains and 1 cm for lithic remains, was georeferenced in three dimensions using
129 X, Y, and Z coordinates and recorded in a GIS database with (vertical and horizontal) spatial
130 distribution data (Moncel et al., 2021).

131 132 2.2. Taphonomy and site formation processes 133

134 The study of site formation processes is an essential step in deciphering the spatial
135 analysis of Palaeolithic sites. Taphonomy has become crucial for distinguishing natural from
136 anthropogenic accumulation processes (Dibble et al., 1997), and assessing how intact
137 assemblages actually are (Henry et al., 2004). As Romagnoli and Vaquero (2016) point out,
138 determining assemblage integrity is a prerequisite for assessing human behaviours through
139 spatial pattern analysis.

140 At the Abri du Maras, taphonomy has been investigated in several studies. Both levels
141 have been described as a well-preserved and almost exclusive anthropogenic accumulation,
142 showing a near absence of animal-induced modification on remains such as digested marks or
143 carnivore and rodent tooth marks (Daujeard et al., 2019; Moncel et al., 2015; Vettese et al.,
144 2022). From a spatial point of view, the evidence of bones in anatomical connections, the
145 lithic and bone refits associated with short-distance connection lines, the absence of
146 significant orientation of material, as well as the scarcity of trampling evidence suggest no
147 major disturbance of archaeological remains (Daujeard et al., 2019; Moncel et al., 2021, 2014;

148 Vignes, 2021) allowing us to conclude that the artefacts have not undergone any major spatial
 149 (horizontal or vertical) displacement (Moncel et al., 2015).

150 However, one particular part of the site shows post-depositional disturbances that have
 151 been identified during fieldwork. Beyond bands 8/9 in the southeast part of the shelter, the site
 152 is partially eroded due to the collapse of the shelter and the development of a small valley in
 153 front of the site. The material in this sector encountered some disturbances and will not be
 154 taken into account for this work.

155
 156

157 2.3. Spatial database

158

159 The lithic database, grouping all the coordinated lithic remains and their characteristics
 160 (length, width, type of rock, typological determination) was intensively exploited for the GIS
 161 spatial analysis of the lithic assemblages. We also used spatial information on charcoal
 162 remains and bone remains. As our research focuses on lithic assemblages, no detailed spatial
 163 analysis of bones was undertaken. We merely visualised the general scattering of bones and
 164 compared them to the more detailed spatial analysis of the lithic material. We also used data
 165 from lithic refits; namely the analysis of lithic refits from level 4.2, as the spatial analysis of
 166 lithic refits from level 4.1 has been published elsewhere (Moncel et al., 2021). Lithic
 167 assemblage composition is quite similar for both levels and mainly composed of flakes and
 168 flake fragments (including in both cases some Levallois flakes), laminar products, points and
 169 cores (Table 1).

170

	Level 4.1	Level 4.2
Flakes (all sizes)	981	984
Flake fragments	340	243
Blades-bladelets	208	100
Points	81	55
Handaxes		1
Cores	51	38
Entire-broken pebbles	32	25
Debris	347	97
Undetermined		72
Total lithic artefacts:	2040	1615
<i>Including tools</i>	<i>50</i>	<i>81</i>
Bone remains	2734	3099
Ash lenses	7	3
Charcoal remains	127	97

171 *Table 1. Technological categories of lithic assemblages and other artefacts from levels 4.1 and 4.2*

172 2.4.3D data

173

174 For the palaeotopographic rendering of the two archaeological levels, we used the 3D

175 point cloud of the Abri du Maras. Laser scanning was carried out during the 2019 campaign

176 using a 360 Light Detection And Ranging (LiDAR) terrestrial laser scanner (Faro Focus).

177 During acquisition, 42 scans were performed. These “scenes” were then assembled, using

178 *3DReshaper* software, into a single point cloud of 70 million points, representing the whole

179 shelter.

180 Since the scan was carried out several years after the excavation of levels 4.1 and 4.2

181 (excavations have currently reached layer 5), the 3D model does not show their respective

182 topographies. Indeed, the 3D survey is carried out at a given moment of the excavation work

183 and gives a 3D image of the surface in its state of progress during the excavation. Therefore,

184 we used the following methodology to reconstruct them in the 3D model of the Abri du

185 Maras.

186

187 **3. Methods**

188

189 3.1.3D palaeotopographic rendering

190

191 The method of palaeotopographic rendering and analysis was carried out in three

192 stages (Fig. 1). We began by cleaning and meshing the point cloud to obtain cleaned surface-

193 based information (Jaillet et al., 2014), more suitable for the next steps. We also performed a

194 rotation and three translations (in X, Y, Z coordinates) to obtain a model in the same

195 coordinate system as the one chosen for excavations at the Abri du Maras.

196 The second stage consisted of surface rendering using the stratigraphic section

197 drawings, which were drawn manually during past excavations and then computerised. Five

198 section drawings were used, showing the stratigraphic limits of the two levels at different

199 locations of the site. We proceeded as follows:

200 1. we created vertical planes georeferenced at the exact location of the section drawings,

201 2. we built texture on these planes by projecting the computerised section drawings

202 (Previously saved as a JPEG file),

203 3. we digitalised points on the stratigraphic limits of the two archaeological levels shown

204 by the projected section drawings,

205 4. the obtained point clouds were then meshed to obtain surface-based information

206 representing the base of each archaeological level.

207 The final step was to analyse the 3D topographies in more detail. We chose to go back

208 to 2D by rasterising them on CloudCompare software (using the average cell height method

209 and a cell size of 0,008 x 0,008 m). This process transforms a 3D surface into a Digital

210 Terrain Model (DTM), which is a digital picture where each pixel contains a value

211 representing elevation information (ESRI, 2016). Finally, we uploaded these DTM files into

212 QGIS software and used the “profile tool” plugin to analyse the topography (Fig. 1). Several

213 longitudinal (west-east) and transversal (north-south) profiles were made on the DTM passing

214 through areas of high material density identified by the spatial analysis, allowing us to study

215 the relationship between archaeological spatial structures and the floor topography during

216 human occupation.

217

218

219

220

221
222
223
224
225
226
227
228
229
230
231
232
233
234
235
236
237
238
239
240
241
242
243
244
245
246
247
248
249
250
251
252
253
254
255
256
257
258
259
260
261
262
263
264
265
266
267
268
269
270

3.2. GIS spatial analysis

The lithic database was imported into QGIS software 3.18 version (QGIS.org, 2021). Due to the high density of artefacts, scattering maps (where each item is represented by a symbol) do not show any clear distribution patterns. We thus used the following method for more in-depth spatial patterning.

3.2.1 General scattering of artefacts: average nearest neighbour

The first step is to statistically characterise the overall scattering of material. Average nearest neighbour is a method used to estimate whether the general pattern is dispersed, clustered or random (de la Torre et al., 2019; Moncel et al., 2021; Sánchez-Romero et al., 2021). If the null hypothesis is rejected, then we can apply “local methods” to identify subzones with clustering or dispersion phenomena (Sánchez-Romero et al., 2021).

3.2.2 Local analysis

Two different local methods were used to ensure the reliable identification of clusters:

- (1) **Kernel density.** This is one of the most common and effective methods (Baxter et al., 1997). It converts a vectorial point layer into a raster heat map where the colour gradient depends on material density. This method calculates the density of point features around each output raster cell (the pixel size was set at 0.01 m, resulting in a low-pixel image with better resolution). A smoothly curved surface is created over each point and spreads to a specific radius around the points. Density value is highest at the point’s location and decreases with increasing distance. It reaches zero at the limit of the search radius distance (set as 0.5 m which is probably the best adapted for our data). The sum of the overlapping Kernel surfaces is then calculated for each pixel (Alperson-Afil, 2008; Alperson-Afil et al., 2009; Oron and Goren-Inbar, 2014; Stavrova et al., 2019). Finally, we standardized densities using maximum values to obtain a uniform scale (from 0 to 1), to facilitate comparisons (Alperson-Afil, 2008; Alperson-Afil et al., 2009, 2007; Coil et al., 2020). Despite the popularity of this method, criticisms of its subjective aspects have emerged (the fact that the analyst has to input a search radius) and of its lack of statistical criteria to identify clusters (Sánchez-Romero et al., 2021; Stavrova et al., 2019).
- (2) **Hotspot analysis.** Recently, statistical methods have become widely used tools for conferring statistical significance on the cluster identification process (de la Torre et al., 2019; Gabucio et al., 2023; Giusti et al., 2018; Mora Torcal et al., 2020; Reeves et al., 2019; Romagnoli and Vaquero, 2016; Sánchez-Romero et al., 2021, 2020, 2016; Spagnolo et al., 2020, 2019; Stavrova et al., 2019). Among the various methods, hotspot analysis, using the Getis-Ord G_i^* statistic (Getis and Ord, 1992; Ord and Getis, 1995), appears to be particularly effective. We used the “Hotspot Analysis” plugin, available on QGIS since 2016 (Oxoli et al., 2018, 2017, 2016). Hotspot analysis detects statistically significant clusters based on quantitative variables and the spatial relationship between artefacts. Qualitative variables must be transformed into quantitative inputs using frequency per quadrats. We created a grid of 0.25 m² quadrats and counted items within each quadrat using the tool “count points in polygon”. Hotspot analysis can then be performed. This method identifies high

271 concentration zones, called hotspots, and low concentration zones, called coldspots.
272 The only prerequisite for this analysis is a sample of at least 30 elements. We
273 systematically compared results with kernel density analysis to assess the proficiency
274 of the QGIS hotspot analysis plugin.
275

276 Using these methods, we started by visualising the general distribution of archaeological
277 finds considering all the lithics, bones and fire-related artefacts. Regarding the latter, it is
278 important to note that no clearly structured hearth has been brought to light at the Abri du
279 Maras. However, studies have shown that burnt artefacts and charcoal distribution can help to
280 identify the locations of “phantom hearths” (Alperson-Afil, 2017, 2008; Alperson-Afil et al.,
281 2007). Moreover, charcoal clusters may indicate dispersed hearths, as fire did not alter the
282 surrounding sediment. Ash lenses can also point to the position of hearths or areas of ash
283 dumping and cleaning. Consequently, we analysed the spatial pattern of fire-related artefacts
284 to locate the position of possible hearths, or at least areas of fire-related activities.

285 Secondly, we carried out analyses by sub-categories of lithic artefacts in order to identify
286 whether specific elements showed a particular pattern compared to others or to overall
287 distribution. Our spatial analysis focuses in particular on stone knapping and the possible
288 identification of the location of reduction sequences. For this purpose, the spatial analysis of
289 Raw Material Units (RMUs) is an effective tool. RMUs incorporate the lithic material from a
290 knapping event, or a series of knapping events carried out for the reduction of a specific
291 nodule (Bargalló et al., 2020b; Chacón et al., 2015; Moncel et al., 2014; Vaquero, 2008;
292 Vaquero et al., 2017). We can thus differentiate pieces brought to the site already knapped
293 (tool kits) (Bargalló et al., 2020a, 2016; Moncel et al., 2021, 2014) from those resulting from
294 *in situ* knapping events. Fifty-two RMUs have been described for level 4.1 (Moncel et al.,
295 2021). Fifteen are composed of pieces introduced to the site already knapped, and a dozen
296 indicate complete or almost complete on-site knapping sequences, with items from all stages
297 of the *chaîne opératoire*. Thus, the spatial patterns of these RMUs may indicate the location
298 of knapping activities and may differ from those of the tool kits. Cortical flakes represent the
299 initial phase of the reduction sequence (Courbin et al., 2020; Oron and Goren-Inbar, 2014), so
300 they may also indicate the place of knapping areas. Lithic refits of level 4.1 have already been
301 published (Moncel et al., 2021), so we only performed the spatial analysis of the lithic refits
302 from level 4.2. They can provide additional information about the knapping activities carried
303 out on site. The examination of the spatial pattern of retouched artefacts is also a critical
304 component of our spatial analysis as tools have already shown potential to characterize
305 activities at the Abri du Maras (Hardy et al., 2013). We also conduct a spatial analysis based
306 on quantitative criteria, such as the length of the artefacts, to determine whether the remains
307 were organised according to their size. In particular, the comparison of these results with the
308 palaeotopographic data may provide taphonomic information.
309

310 4. Results

311

312 4.1. General scattering of artefacts

313

314 Nearest neighbour analysis was carried out to characterise the overall scattering of
315 archaeological finds in levels 4.1 and 4.2. This statistical test was applied to all remains, and
316 shows that spatial distribution is significantly clustered (all remains from level 4.1: score $z = -$
317 55.9 , p value < 0.01 ; all remains from level 4.2: score $z = -63.1$, p value < 0.01). We also
318 applied this test to the three main categories of artefacts separately (level 4.1: lithics: score $z =$
319 -32.7 , p value < 0.01 ; bones: score $z = -41.7$, p value < 0.01 ; charcoal remains: score $z = -$

320 7.24, p value < 0.01 ; level 4.2: lithics: score $z = -34.7$, p value < 0.01 ; bones: score $z = -$
321 49.9, p value < 0.01 ; charcoal remains: score $z = -8.42$, p value < 0.01);. In all cases, spatial
322 scattering is statistically clustered.

323

324 4.2. General patterns of lithics, bones and fire-related artefacts in level 4.1

325

326 The hotspot analysis of level 4.1 (Fig. 2) shows that lithic, bone and charcoal clusters
327 overlap in the same areas, especially in the north-eastern part of the excavated zone, except
328 for square I5, where no charcoal concentrations were found. Likewise, kernel density shows
329 the same results (Fig. S1). Statistically significant clusters of charcoals appear to be closely
330 spatially related to the densest accumulations of burnt artefacts (Fig. 2C). Charcoal and ash
331 lenses are observed in areas with high concentrations of lithics and bones.

332 Thus, the main clusters of bones and lithics and indicators of fire activities are
333 concentrated in the north and north-eastern part of level 4.1. Our analysis, therefore, shows
334 that these were probably the main activity areas in level 4.1.

335

336 4.3. Spatial patterns associated with typo-technological aspects of level 4.1

337

338 RMU flint-13 ($n=231$) and RMU quartz-5 ($n=40$) are the largest RMUs and include
339 artefacts from all stages of the on-site *chaîne opératoire*. They are located in the previously
340 identified main accumulation areas (Fig. 3), where most of the lithics, bones and charcoals are
341 clustered. Kernel densities reveal the same spatial distributions (Fig. S2).

342 Eight out of the 10 RMUs with evidence of on-site *chaîne opératoires* show
343 preferential concentrations in the same areas (square I5-I6 and the north-eastern part of band
344 6). These patterns may indicate that the main knapping areas were the northern and north-
345 eastern parts of the site. For the other two RMUs, cluster distribution (Fig. S3 and S4) appears
346 to indicate secondary knapping areas in the western and south-western parts of the site.

347 Fifteen RMUs, made up of 26 pieces, contain artefacts brought to the site already
348 knapped (tool kits). Only kernel density analysis can be performed because they incorporate
349 less than 30 pieces. Their spatial distributions indicate a more random pattern than the
350 previous RMUs (Fig. 4). They seem to be scattered over the whole site without preferential
351 accumulation areas. This confirms that spatial patterns differ for items from *in situ* knapping
352 events and pieces introduced to the site already knapped.

353 Cortical flakes are clustered in the main accumulation areas confirming that knapping
354 activities probably took place in this part of the site (Fig. 5). Kernel density shows the same
355 results (Fig. S5).

356 Figure 6 shows that lithic tools are found in square I5 and also a little in M6, areas
357 already identified for their cluster of lithics. However, the rest of the lithic tool spatial analysis
358 displays a different pattern to those previously highlighted, which is confirmed by kernel
359 density (Fig. S6). A significant cluster of tools is located in the middle of the excavated area,
360 where no other cluster has been found. Very few retouched artefacts are found in the north-
361 eastern part, where most lithics, bones and charcoals are located.

362 Several statistically significant clusters of large and small pieces were detected (Fig.
363 7). In the northwest, a cluster of large pieces (hotspot H1) was brought to light in an area
364 where no particular accumulation had yet been identified. The second hotspot (H2) is mainly
365 in square J7, where part of the lithic tools is located. The last hotspot (H3) is located in the
366 eastern part of the site, south of the largest concentration of lithic remains. Two coldspots
367 (clusters of small pieces) were identified. The larger one is located in the main concentration
368 of lithic artefacts. A second coldspot (C2) to the south of H3 is composed of fewer pieces.

369 The composition of the aforementioned clusters confirms length differences between hotspots
370 and coldspots (Table S1).

371

372 *4.4. General patterns of lithics, bones, and fire-related artefacts in level 4.2*

373

374 We performed the same analyses than level 4.1 to identify the main activity areas in
375 level 4.2. The hotspot analysis of lithics, bones and charcoals displays two main cluster areas.
376 The most extensive one is in the north-eastern part, and the second one is in the northwest of
377 the excavated area (Fig. 8). The largest charcoal cluster is in the western part. Kernel density
378 shows the same results as hotspot analysis (Fig. S7).

379 Burnt lithic clusters overlap with charcoal and ash lenses (Fig. 8C). Fire-related
380 artefacts are closely spatially related and are located in the main clusters of lithics and bones.

381

382 *4.5. Spatial patterns associated with typo-technological aspects of level 4.2*

383

384 We carried out a detailed spatial analysis of the upper level 4.2. Many lithics from this
385 level have been refitted but data from RMU analysis are still being processed.

386 Hotspot analysis (Fig. 9) and kernel density (Fig. S8) show that cortical flakes are
387 clustered in the western part of the site. No dense zone, or meaningful cluster, is visible in the
388 northeast, among the largest concentration of lithic artefacts. As mentioned above, we did not
389 focus on the southeast of the site (from squares K9-L9-M9-N9) as it has undergone extensive
390 post-depositional disturbances.

391 Out of a total of 1615 lithic remains from level 4.2, 81 are retouched artefacts.
392 Statistically significant clusters are found in the western part of the site (Figs. 10 and S9),
393 whereas no tool clusters are visible in the eastern part of level 4.2, where the highest
394 concentrations of lithics and bones are found. However, lithics, bones and charcoals are also
395 clustered in the western part of the site. Lithic tools are concentrated on the margins of those
396 clusters, rather than in them.

397 The spatial analysis of cores also shows clustering in the west of the site (Figs. 11 and
398 S10) and no statistical concentrations in the northeast, where the most significant clusters of
399 remains are located.

400 We performed hotspot analysis according to artefact length to shed more light on these
401 patterns (Fig. 12). Three clusters of large pieces can be identified, two of which are in the
402 disturbed area. The first hotspot (H1) is located in the northwest of the site, close to where
403 cores, tools, and clusters of lithics, bones and charcoals are found. Two other hotspots (H2
404 and H3) are in the disturbed area of the site. A significant cluster of small artefacts (coldspot
405 C1) is located in the north-eastern part of the site, where the highest concentration of lithics
406 and bones was already identified. This area is thus mainly composed of small pieces, and no
407 large pieces are found in this zone. A second coldspot (C2) is in the disturbed part of the site.
408 The composition of the clusters confirms length differences between hotspots and coldspots
409 (Table S2).

410 Level 4.2 comprises 22 refit groups, for a total of 53 pieces, with 29 connection lines
411 (Fig. S11, Table S3). Most of the refits are in the main accumulation areas (northeast of the
412 site) and only two refits are in the western part of the excavated area (Fig. S11). Most of the
413 connection lines are between 0 and 2 m and are within the normal dispersion range for on-site
414 knapping sequences, as shown by experimental archaeology (Cziesla, 1990; Moncel et al.,
415 2021, 2014; Vaquero et al., 2019, 2017). Four connection lines are beyond 2 m and could
416 suggest the intentional anthropogenic displacement of some pieces during daily activities.

417

4.6. *Palaeotopography of level 4.1*

The topography of the base of the surface of level 4.1 was rendered in 3D. Most of the area was successfully interpolated, bringing to light the general topography of the level. Fig. 13A shows the dip in an altitude-dependent colour scale. The 4.1 surface shows downward dips from the northwest to the southeast, probably due in part to the compression and compaction of sediment over time. The highest elevation in the northwest corner is about -2 m above level 0, and the lowest in the southeast corner is almost -3.60 m.

The DTM and the QGIS "profile tool" plugin allow us to study the topography in more detail (Fig. 13B). Several longitudinal (west-east) and transversal (north-south) profiles were made on the DTM, passing through clusters of small and large lithic artefacts previously identified. The longitudinal sections show a slight, progressively decreasing west-east dip, with a steeper slope in the western part, clearly visible on profiles BB' and CC' (at bands E, F and G). Beyond these bands, the dip is negligible or even non-existent, as shown in the eastern half of profile CC'. The difference in elevation from one end to the other is 1 m maximum. The transversal profiles (DD' and EE') show a north-south dip, steeper than the west-east dip, with a negative gradient of almost 1 m over a distance of 3 m (section DD'). However, the slope rises slightly in the middle (band 7) and falls again.

4.7. *Palaeotopography of level 4.2*

In the upper level, 3D rendering was successful for most of the area, but part of the eastern trench could not be entirely interpolated. Nevertheless, this surface provides general information on the northwest to southeast dipping topography of level 4.2 (Fig. 14A).

In QGIS, profiles were made on the DTM (Fig. 14B) and deliberately run through clusters of small and large remains to detail the topography in these areas. The W-E profiles show a gradual decrease in dip from west to east, with an altitude differential of about 1 m from one end to the other. In the western part of the site, the DD' profile shows a very slight north-south dip in the first part, followed by significant steepening of the slope and subsequent stabilising. In the eastern part, the dip decreases progressively from north to south and then significantly, with an altitudinal difference of 90 cm over a distance of 4 metres (section CC'). However, the slope rises slightly and decreases significantly again towards the centre of the surface (visible on profile EE'). The southern ends of profiles CC' (from square M9) and EE' (from square L9) correspond to the beginning of the disturbed area.

5. Discussion

5.1. *Site formation processes*

Site formation processes have to be considered when performing spatial analysis. It is a prerequisite for assessing human behaviours through spatial patterns (Romagnoli and Vaquero, 2016). As previously said, many studies have shown that both levels are well-reserved anthropogenic accumulations, with a lack of post-depositional disturbances (Daujeard et al., 2019; Moncel et al., 2021, 2015, 2014; Vettese et al., 2022; Vignes, 2021).

Our analysis completes those results. The combination of spatial analysis and topographic data is a powerful tool that can help to assess site formation processes. Indeed, disturbances, such as runoff or water flow, can alter the spatial distribution of remains, causing movement and downslope displacement (Petraglia and Potts, 1994). Spatial analysis and palaeotopographic rendering of levels 4.1 and 4.2 do not show such patterns. The areas

467 with the highest artefact density are located in the northern part of the site and follow a gentle
468 slope. In contrast, the lowest areas (south and southeast of the site) contain fewer remains and
469 no significant clusters of material. This pattern is general across the site and for both levels,
470 the areas of highest densities are found in the highest part of the site, east and west, while
471 towards the south, the artefact densities are much lower. Thus, the material is not located in
472 the more depressed areas and is not organised following the slope, which would have been
473 observed if levels had encountered spatial disturbances caused by water for example. In
474 addition, water flows tend to sort archaeological remains by size (Dibble et al., 1997; Gabucio
475 et al., 2023; Petraglia and Potts, 1994; Sánchez-Romero et al., 2020) with displacements of
476 large pieces into hollows and the removal of smaller remains from the assemblage. Both
477 archaeological levels comprise clusters of small items that are found in the northern part of
478 the site, areas with gentle slopes. For level 4.1, section EE' has a slight depression and the
479 majority of the cluster of large lithic artefacts is not located in the deepest part, but at the
480 margins of this depressed zone. Thus, we can say that, for both levels, clusters of large pieces
481 are not in the lowest or most depressed part of the site. The proximity of the large and small
482 artefact clusters, especially for level 4.1, also indicates the absence of significant spatial
483 disturbance, such as water flows.

484 Another important issue and a common feature of Palaeolithic sites is the palimpsest
485 problem (e.g., Bailey, 2007; Galanidou, 2000; Henry, 2012; Machado et al., 2019, 2013;
486 Malinsky-Buller et al., 2011; Mallol and Hernández, 2016; Mora Torcal et al., 2020; Picin and
487 Cascalheira, 2020; Reeves et al., 2019; Vaquero, 2008; Vaquero et al., 2012; Vaquero and
488 Pastó, 2001). Both levels are palimpsests of several occupations (Moncel et al., 2021, 2015),
489 meaning that Neanderthals possibly occupied the same areas repeatedly during short-term
490 stays in the shelter. Multiple short-term occupations of the same site during a short period of
491 time are a common characteristic of Middle Palaeolithic sites (for this specific topic see
492 Cascalheira and Picin, 2020). In those cases, vertical plots are commonly used to decipher
493 palimpsests (e.g., Bargalló et al., 2020, 2016; Coil et al., 2020; Mora Torcal et al., 2020;
494 Sañudo et al., 2012; Vaquero, 2008; Vaquero and Pastó, 2001) and although this paper
495 focuses primarily on horizontal analysis, we also visualised vertical dispersion (Guillemot
496 2021). But it was not possible to untangle any palimpsests.

497 However, in some cases, palimpsests are not necessarily an issue. Indeed, the rapid
498 burial of the levels at the Abri du Maras (Moncel et al., 2021), makes them “rapid-
499 accumulation palimpsests” (Malinsky-Buller et al., 2011). According to this model, spatial
500 patterns and anthropogenic clusters can still be observed even though these two sub-levels are
501 palimpsests. Moreover, following the idea of Reeves et al., (2019), palimpsests should not
502 only be viewed as a hindrance to spatial analysis but on the contrary, can be a necessary
503 condition for identifying behaviours. Bailey and Galanidou (2009) already suggested that
504 palimpsests, especially in caves or rock shelters, have a great potential to give information
505 about the use of space. The fact that the same rock shelter was used many times for many
506 short-term occasions and probably by the same groups tends to create patterns that are
507 repeated over time. This is mainly due to the physical conditions of caves and rock shelters
508 (walls, ceiling, interior versus exterior...) that influenced the way of using space, and the fact
509 that palimpsests create a living space where remains of past occupations may influence
510 subsequent occupations (Bailey and Galanidou, 2009). Thus, these characteristics probably
511 influence the way of re-using the same space, especially if the occupations are of similar
512 duration. Following that idea, palimpsest does not hinder patterns but creates them. However,
513 even if palimpsest makes patterns distinguishable, we must keep in mind that the different
514 clusters may not be contemporaneous.

515

516 5.2. *Significance of level 4.1 spatial patterns*
517

518 The hotspot analysis of level 4.1 identified several main activity areas associated with
519 peripheral areas (Fig. 15A). The largest clusters of lithics, bones and fire-related remains are
520 concentrated in the north-eastern part of the site. The analysis of cortical flakes and RMUs
521 shows that *in situ* knapping activities took place there. This is confirmed by the presence of
522 clusters of lithic refits in this area, with connection lines within the normal dispersion range
523 for on-site knapping sequences (Moncel et al., 2021). Metrical analysis indicates that this area
524 includes small flakes, which are a reliable indicator of the location of knapping activities
525 (Henry et al., 2004; Sañudo et al., 2012; Vaquero et al., 2001; Vaquero and Pastó, 2001). All
526 the analyses point to areas dedicated to knapping activities and surrounded by some clusters
527 of lithic tools and large lithic artefacts (Fig. 15A). Those types of remains have been
528 described as artefacts moved from the main activity areas to the peripheries (Vaquero et al.,
529 2001).

530 This pattern can be compared to the "drop-toss area" model observed among modern
531 hunter-gatherers (Binford, 1983). According to Binford, knapping activities are concentrated
532 in areas around hearths. These areas mainly contain small pieces ("drop zone"). The reason
533 for this is that large pieces, which could potentially hinder the continuation of the activity or
534 are required for use elsewhere, are moved to peripheral areas ("toss zone"). Level 4.1 of the
535 Abri du Maras displays similar spatial patterns. No hearth has been identified but ash lenses,
536 charcoal remains, burnt lithics and their spatial relationship indicate fire-related activities and
537 perhaps the location of short-lived hearths that did not alter the surrounding sediments.
538 Studies have already shown that fire-related artefacts can attest to 'phantom hearths'
539 (Alperson-Afil, 2017, 2008; Alperson-Afil et al., 2007). The knapping areas in level 4.1 seem
540 to be closely related to fire-related activities.

541 The particular case of square I5 should be mentioned. While showing evidence of a
542 drop zone (cluster of cortical flakes, cluster of RMU showing knapping activities and
543 presence of refits), this square also displays a cluster of tools. Length analysis is not helpful as
544 the results do not show statistical evidence for clusters of small or large artefacts. This
545 mixture of features may be due to palimpsests and illustrates that some parts of the site may
546 be difficult to understand due to repeated short-term occupations. This could also explain the
547 presence of few lithic tools in M6.

548 This paper focuses almost exclusively on lithic material and it is thus difficult to
549 define spatial organisation in greater detail. Level 4.1 contains evidence of intense specialised
550 reindeer butchery activities (Daujeard et al., 2019; Moncel et al., 2021), showing that all the
551 stages of the butchery *chaîne opératoire* were carried out *in situ* (Daujeard et al., 2019;
552 Vettese et al., 2017). A high-resolution spatial analysis of the faunal remains will be required
553 to complete our conclusions.
554

555 5.3. *Significance of level 4.2 spatial patterns*
556

557 The spatial organisation of level 4.2 is different to that of level 4.1 (Fig. 15B). We
558 identified two main accumulation areas, possibly related to the aspect of the shelter. It is
559 important to recall that the shelter may have been slightly larger during occupations of level
560 4.2 than level 4.1. Neanderthals could have occupied the site differently, extending activities
561 over a larger surface. Another explanation could be the extension of level 4.2 excavations.
562 Indeed, compared to the above level, level 4.2 was excavated over a larger area, which could
563 generate a bias in the understanding of the site and give the impression that Neanderthals
564 occupied the shelter over a larger surface.

565 Area 1 presents the most significant clusters of lithics and bones. Further investigation
566 showed that this area contains mainly small artefacts. Moreover, most of the lithic refits are
567 from this area, with most connection lines in the normal dispersion range for on-site knapping
568 sequences (Cziesla, 1990; Moncel et al., 2021, 2014; Vaquero et al., 2019, 2017). As with the
569 upper level, these two characteristics appear to reveal an area used for knapping activities.
570 Area 2, located in the western part of the site, comprises smaller clusters of lithics and bones
571 but also contains the largest cluster of charcoals. This area includes clusters of lithic tools,
572 cores and large artefacts. With just two refits and no clusters of small remains, it is unlikely
573 that the western part of level 4.2 was a central location of knapping activities. Both areas
574 attest to fire-related items, even though more intense fire activities seem to have taken place
575 in Area 2, as shown by the higher density of charcoals. Finally, squares I6 and J6 are
576 intriguing. They are located at the boundary of Area 1, but clusters of cores, cortical flakes
577 and lithic tools can be observed in this zone.
578 Binford's model seems less relevant here as it would predict more fire-related artefacts and
579 cortical flakes in Area 1, where knapping activities have been identified. Without data on
580 RMUs, it is difficult to describe the spatial patterning of this level in more detail. However,
581 we clearly observe the distribution of different types of artefacts in distinct areas, and these
582 two areas attest to very different typo-technological characteristics. The absence of refits
583 connecting them confirms the organisation of level 4.2 into two different zones, and perhaps
584 different and unrelated phases of site occupation. Moreover, an initial spatial analysis of
585 faunal remains has identified a different pattern between ungulate types and according to
586 anatomical elements. While the remains of large-sized ungulates (horse, bison, megaceros), as
587 well as cranial and post-cranial axial skeletons, seem to be more densely concentrated in Area
588 1, the bones of medium-sized ungulates (reindeer, red deer), and the remains of the
589 appendicular skeletons are more concentrated in Area 2 (Vignes, 2021). This may confirm the
590 spatial organisation of level 4.2 into two distinct areas, or unrelated phases of occupation.
591

592 5.4. *The Abri du Maras in the Middle Palaeolithic cultural context* 593

594 The spatial analysis of Middle Palaeolithic sites is an integral component of debates on
595 the complexity of Neanderthal behaviour and social organisation (e.g., Anderson and Burke,
596 2008; Henry et al., 2004; Oron and Goren-Inbar, 2014; Pettitt, 1997; Vaquero et al., 2001;
597 Vaquero and Pastó, 2001). For many years, no complex spatial organisation was found for
598 Middle Palaeolithic sites (Alperson-Afil and Hovers, 2005), sometimes due to the inherent
599 difficulties in understanding palimpsests. This has led some authors to consider that
600 Neanderthal social organisation was less complex than that of Modern Humans (Oron and
601 Goren-Inbar, 2014).

602 However, that idea has now come under strong criticism, and some authors view
603 Middle Palaeolithic spatial structures as indicative of complex organisation, similar to that of
604 *Homo sapiens*. At the Abric Romaní (Spain, levels H, I, J, K and L dated between 45 to 52
605 ka), the spatial layout of Neanderthal activities fits the model of hearth-related assemblages,
606 with knapping activities systematically carried out near hearths (Vaquero et al., 2001;
607 Vaquero and Pastó, 2001). The Jordanian Tor Faraj site (floors I and II, average age of $55.1 \pm$
608 5.6 ka) is spatially organised in a complex way, with butchery areas, final lithic and food
609 processing areas, initial lithic processing areas and bedding areas (Henry, 2012; Henry et al.,
610 2004). At the Amud Cave site in Israel (55 to 69 ka), sub-unit B2 comprises knapping areas
611 and specific zones for the disposal of unusable lithic materials (Alperson-Afil and Hovers,
612 2005). In levels 2.2 and 3 of the Crimean site of Karabi Tamchin (MIS 3), a differential use of
613 space was observed according to activities (discard areas, tool manufacturing, bone
614 processing and tool use areas) (Anderson and Burke, 2008). Level VII of the Amalda I Cave

615 (Spain, between ca 42 600 and 44 500 uncal BP) reveals a different spatial layout in keeping
616 with artefact type and the length of remains (Sánchez-Romero et al., 2020). The spatial
617 organisation of the Israeli open-air site of Quneitra (53 ± 5.9 ka BP) is delimited by knapping,
618 butchering or marrow extraction activities (Oron and Goren-Inbar, 2014).

619 Our analysis indicates that the Neanderthal groups of the Abri du Maras structured the
620 spatial management of the shelter, with main activity areas used for intense knapping
621 activities and associated with fire-related activities. Other areas with specific remains, such as
622 the largest pieces or lithic tools, were located elsewhere. These behaviours are similar to those
623 described above; the inhabited space is structured by the type of remains and probably by the
624 type of activities. It is important to emphasise that the spatial pattern of level 4.2 is slightly
625 different and more difficult to interpret than level 4.1, perhaps because the shelter was
626 occupied over a larger area or because activities were different. It is important to remember
627 that while the lithic industry is similar for both levels, the faunal assemblage of level 4.2 is
628 more diverse (Daujeard et al., 2019) perhaps reflecting a different type of occupation. The
629 palaeotopographic reconstructions for the two levels do not show significant differences (a
630 decreasing slope from northwest to southeast for both levels), and the inter-level variation of
631 the spatial organisation was probably dictated by the social organisation or cultural choices of
632 Neanderthal groups, such as types of activities, and not by a change in soil topography. Inter-
633 level variations have already been observed for Middle and Upper Palaeolithic sites (e.g.,
634 Anderson and Burke, 2008; Caron-Laviolette et al., 2018; Vaquero et al., 2001). A recent
635 study on butchery tradition indicates that different marrow extraction methods occurred
636 between levels 4.1 and 4.2 (Vettese et al., 2022), suggesting that the shelter was used by
637 distinct groups with their own tradition and perhaps different group compositions or structures
638 (more or less specialized Neanderthals). This may explain the difference in the spatial pattern
639 between levels, both groups occupied the site differently. This variation in spatial organisation
640 between sub-levels has yet to be confirmed by further analysis, especially spatial studies of
641 faunal remains, level 4.2 RMU analysis and high-resolution vertical spatial analysis.

642
643

644 5.5. *Methodological aspects*

645

646 We wanted to demonstrate the efficiency of a spatial analysis carried out under a free
647 and open source GIS software. While some authors have stressed the need to use such open
648 source software in order to ensure a healthier scientific practice (Ducke, 2012; Ince et al.,
649 2012; Morin et al., 2012), others have shown the advantages of open source GIS software
650 over proprietary software for archaeological research (Orengo, 2015). This is especially
651 important in a context where GIS has become an indispensable tool for archaeologists
652 (Brouwer Burg, 2017; Howey and Brouwer Burg, 2017; Orengo, 2015; Richards-Rissetto,
653 2017; Whitley, 2017). So far, hotspot analyses have only been carried out using commercial
654 software, including ArcGIS (Mora Torcal et al., 2020; Sánchez-Romero et al., 2021, 2020;
655 Stavrova et al., 2019). Our analysis shows the relevance of performing hotspot analysis using
656 an open source software. We systematically compared hotspot results with kernel density
657 analysis to test the reliability of the plugin and confidently identify clusters by combining
658 methods (Sánchez-Romero et al., 2021). Both methods gave the same results, thus, the QGIS
659 “Hotspot Analysis” plugin appears to be an appropriate free and open source tool for studying
660 spatial patterns.

661 Palaeotopographic reconstruction is a valuable tool to help investigate the spatial
662 distribution of archaeological remains (Bargalló et al., 2020a; Gabucio et al., 2023; Sánchez-
663 Romero et al., 2020). Combined with high-resolution spatial analysis, it provides detailed
664 behavioural and taphonomic information. The 3D method used in this paper is not just a

665 digitisation of archaeological surfaces but a reconstruction of parts of the site, which no
666 longer existed when the laser scanning of the Abri du Maras was carried out. We have used
667 available section drawings to reconstruct ancient topographies. While this method seems
668 efficient, we must to emphasize that the reconstructed surfaces are imperfect, as some parts
669 could not be interpolated correctly. This was due to the limited number of useful section
670 drawings that have been used (some being unavailable to record or to use by the quantity of
671 blocks due to the final collapse of the shelter). That point is essential because even if the
672 reconstructed topographies seem coherent, we would have needed more stratigraphic section
673 drawings, spread over the whole site area, for homogeneous, complete and more precise
674 rendering.

675 Finally, we would like to highlight the complementarity between 2D and 3D analyses.
676 Once the palaeosurfaces had been rendered in 3D, we chose to go back to 2D by analysing
677 them with QGIS. In our view, the possibilities of 2D-3D back and forth have not been
678 sufficiently underlined, even though the potentialities of "GIS + 3D" have already been
679 discussed (Dell'Unto and Landeschi, 2022). 3D technologies offer access to new types of
680 analysis and ultimately to a better understanding of archaeological sites (Campana, 2016;
681 Westoby et al., 2012). At the same time, the development of GIS has led to significant
682 advances in how we visualise, process and analyse archaeological data (McCoy and
683 Ladefoged, 2009). But when used together, 2D and 3D methods offer excellent tools for the
684 high-resolution spatial analysis of archaeological sites and the reconstruction of the daily
685 activities of past human groups.

686
687

688 **6. Conclusion**

689

690 The primary goal of this research was to perform a high-resolution spatial analysis of
691 the lithic assemblages of levels 4.1 and 4.2 (MIS 3) from the Abri du Maras. By combining
692 2D analyses, using a free and open-source GIS software, and 3D palaeotopographic
693 reconstructions we were able to provide evidence about the use of space by Neanderthals. We
694 have to keep in mind that both levels are palimpsests. However, even if Neanderthals
695 repeatedly occupied the shelter in a short period of time, it is still possible to identify spatial
696 patterns.

697 Spatial management is well-defined in level 4.1, where the main areas were used for
698 knapping and probably associated with fire activities. Specific remains, such as large pieces or
699 lithic tools were located on the periphery of these main areas. The spatial pattern in level 4.2
700 was somewhat different and not as clear, with two main distinct accumulation areas related to
701 specific typo-technological composition. Those inter-level variations of spatial organisation
702 do not appear to be dictated by a change in soil topography but probably by cultural choices,
703 activities or different ways of occupying the shelter surface (perhaps because the shelter was
704 larger and occupied over a larger area). Our analysis also furnishes new evidence on site
705 formation processes and confirms that levels at the Abri du Maras were not subject to intense
706 post-depositional disturbances. These observations point to a complex organisation at the Abri
707 du Maras, with a structured division of space according to the types of remains and probably
708 the types of activities. These behaviours are similar to those described in modern hunter-
709 gatherer models and to those observed in other Middle Palaeolithic sites with complex social
710 organisations.

711 Future analyses, currently under study, particularly of level 4.2, may provide
712 additional information to better understand the occupational patterns of some of the last
713 Neanderthal groups in the Rhône Valley.

714

715
716
717
718
719
720
721
722
723
724
725
726
727
728
729
730
731
732
733
734
735
736
737
738
739
740
741
742
743
744
745
746
747
748
749
750
751
752
753
754
755
756
757
758
759
760
761
762
763
764

Acknowledgements

Fieldwork was backed by the Service de l'Archéologie, Région Auvergne-Rhône-Alpes, French Ministry of Culture.

The analyses were financed by the Museum National d'Histoire naturelle, and the CERP (Tautavel, France). M.G.CH.'s research is funded by Research Group n° 2017 SGR 836 of the Catalan Government, project PID2019-103987GB-C31) of the Ministry of Science and Innovation, CERCA Programme/Generalitat de Catalunya and the "Spanish Ministry of Science and Innovation through the 'María de Maeztu' program for Units of Excellence (CEX2019-000945-M).

3D analysis was carried out at the Pôle Images 5D of the Laboratoire EDYTEM.

The English manuscript was edited by L. Byrne, an official translator and native English speaker.

We thank the editor and the reviewers for their useful comments that enriched and improved our paper.

Declarations of interest: none

References

Alperson-Afil, N., 2017. Spatial Analysis of Fire: Archaeological Approach to Recognizing Early Fire. *Current Anthropology* 58, S258–S266. <https://doi.org/10.1086/692721>

Alperson-Afil, N., 2008. Continual fire-making by Hominins at Gesher Benot Ya'aqov, Israel. *Quaternary Science Reviews* 27, 1733–1739. <https://doi.org/10.1016/j.quascirev.2008.06.009>

Alperson-Afil, N., Hovers, E., 2005. Differential use of space at the Neandertal site of Amud Cave, Israel. *Eurasian Prehistory* 3, 3–22.

Alperson-Afil, N., Richter, D., Goren-Inbar, N., 2007. Phantom hearths and the use of fire at Gesher Benot Ya' Aqov, Israël. *PaleoAnthropology* 7, 1–15.

Alperson-Afil, N., Sharon, G., Kislev, M., Melamed, Y., Zohar, I., Ashkenazi, S., Rabinovich, R., Biton, R., Werker, E., Hartman, G., Feibel, C., Goren-Inbar, N., 2009. Spatial Organization of Hominin Activities at Gesher Benot Ya'aqov, Israel. *Science* 326, 1677–1680. <https://doi.org/10.1126/science.1180695>

Anderson, K.L., Burke, A., 2008. Refining the definition of cultural levels at Karabi Tamchin: a quantitative approach to vertical intra-site spatial analysis. *Journal of Archaeological Science* 35, 2274–2285. <https://doi.org/10.1016/j.jas.2008.02.011>

Bailey, G., 2007. Time perspectives, palimpsests and the archaeology of time. *Journal of Anthropological Archaeology* 26, 198–223. <https://doi.org/10.1016/j.jaa.2006.08.002>

Bailey, G., Galanidou, N., 2009. Caves, palimpsests and dwelling spaces: examples from the Upper Palaeolithic of south-east Europe. *World Archaeology* 41, 215–241. <https://doi.org/10.1080/00438240902843733>

765
766 Bargalló, A., Gabucio, M.J., Gómez de Soler, B., Chacón, M.G., Vaquero, M., 2020a. A
767 Snapshot of a Short Occupation in the Abric Romaní Rock Shelter: Archaeo-Level Oa, in:
768 Cascalheira, J., Picin, A. (Eds.), *Short-Term Occupations in Paleolithic Archaeology,*
769 *Interdisciplinary Contributions to Archaeology.* Springer International Publishing, Cham,
770 pp. 217–235. https://doi.org/10.1007/978-3-030-27403-0_9
771
772 Bargalló, A., Gabucio, M.J., Rivals, F., 2016. Puzzling out a palimpsest: Testing an
773 interdisciplinary study in level O of Abric Romaní. *Quaternary International, Advances in*
774 *Palimpsest Dissection 417*, 51–65. <https://doi.org/10.1016/j.quaint.2015.09.066>
775
776 Bargalló, A., Gabucio, M.J., Soler, B.G. de, Chacón, M.G., Vaquero, M., 2020b.
777 Rebuilding the daily scenario of Neanderthal settlement. *Journal of Archaeological*
778 *Science: Reports 29*, 102139. <https://doi.org/10.1016/j.jasrep.2019.102139>
779
780 Baxter, M.J., Beardah, C.C., Wright, R.V.S., 1997. Some archaeological applications of
781 kernel density estimates. *Journal of Archaeological Science 24*, 347–354.
782
783 Binford, L.R., 1983. *In pursuit of the past: decoding the archaeological record.* Thames
784 and Hudson, London.
785
786 Brouwer Burg, M., 2017. It must be right, GIS told me so! Questioning the infallibility of
787 GIS as a methodological tool. *Journal of Archaeological Science 84*, 115–120.
788 <https://doi.org/10.1016/j.jas.2017.05.010>
789
790 Campana, S. (Ed.), 2016. *Proceedings of the 43rd Annual Conference on Computer*
791 *Applications and Quantitative Methods in Archaeology,* Archaeopress archaeology.
792 Archaeopress Publishing Ltd, Oxford.
793
794 Caron-Laviolette, E., Bignon-Lau, O., Olive, M., 2018. (Re)occupation: Following a
795 Magdalenian group through three successive occupations at Étioilles. *Quaternary*
796 *International 498*, 12–29. <https://doi.org/10.1016/j.quaint.2018.10.043>
797
798 Cascalheira, J., Picin, A. (Eds.), 2020. *Short-Term Occupations in Paleolithic*
799 *Archaeology: Definition and Interpretation,* *Interdisciplinary Contributions to*
800 *Archaeology.* Springer International Publishing, Cham. [https://doi.org/10.1007/978-3-](https://doi.org/10.1007/978-3-030-27403-0)
801 [030-27403-0](https://doi.org/10.1007/978-3-030-27403-0)
802
803 Chacón, M.G., Bargalló, A., Gabucio, M.J., Rivals, F., Vaquero, M., 2015. Neanderthal
804 Behaviors from a Spatio-Temporal Perspective: An Interdisciplinary Approach to
805 Interpret Archaeological Assemblages, in: Conrad, Nicolas.J. (Ed.), *Settlement Dynamics*
806 *of the Middle Paleolithic and Middle Stone Age,* Tübingen Publications in Prehistory.
807 Kerns, Tübingen, pp. 253–294.
808
809 Coil, R., 2016. *Spatial approaches to site formation and carnivore-hominin interaction at*
810 *Dmanisi, Georgia.* (Ph.D. Dissertation). University of Minnesota.
811
812 Coil, R., Tappen, M., Ferring, R., Bukhsianidze, M., Nioradze, M., Lordkipanidze, D.,
813 2020. Spatial patterning of the archaeological and paleontological assemblage at Dmanisi,
814 Georgia: An analysis of site formation and carnivore-hominin interaction in Block 2.

815 Journal of Human Evolution 143, 102773. <https://doi.org/10.1016/j.jhevol.2020.102773>
816
817 Comber, J., 1967. Le Paléolithique de l'Ardèche dans son cadre bioclimatique.
818 Imprimerie Delmas, Bordeaux.
819
820 Courbin, P., Brenet, M., Michel, A., Gravina, B., 2020. Spatial analysis of the late Middle
821 Palaeolithic open-air site of Bout-des-Vergnes (Bergerac, Dordogne) based on lithic
822 technology and refitting. *Journal of Archaeological Science: Reports* 32, 102373.
823 <https://doi.org/10.1016/j.jasrep.2020.102373>
824
825 Cziesla, E., 1990. On refitting of stone artifacts, in: Cziesla, E., Eickhoff, S., Arts, N.,
826 Winter (Eds.), *The Big Puzzle. International Symposium on Refitting Stone Artefacts.*
827 *Studies in Modern Archaeology, Holos, Bonn*, pp. 9–44.
828
829 Daujeard, C., Vettese, D., Britton, K., Béarez, P., Boulbes, N., Crégut-Bonnoure, E.,
830 Desclaux, E., Lateur, N., Pike-Tay, A., Rivals, F., Allué, E., Chacón, M.G., Puaud, S.,
831 Richard, M., Courty, M.-A., Gallotti, R., Hardy, B., Bahain, J.J., Falguères, C., Pons-
832 Branchu, E., Valladas, H., Moncel, M.-H., 2019. Neanderthal selective hunting of
833 reindeer? The case study of Abri du Maras (south-eastern France). *Archaeol Anthropol*
834 *Sci* 11, 985–1011. <https://doi.org/10.1007/s12520-017-0580-8>
835
836 de la Torre, I., Vanwezer, N., Benito-Calvo, A., Proffitt, T., Mora, R., 2019. Spatial and
837 orientation patterns of experimental stone tool refits. *Archaeol Anthropol Sci* 11, 4569–
838 4584. <https://doi.org/10.1007/s12520-018-0701-z>
839
840 Debard, E., 1988. Le Quaternaire du Bas-Vivarais d'après l'étude des remplissages
841 d'avens, de porches de grottes et d'abris sous roche. *Dynamique sédimentaire,*
842 *paléoclimatologie et chronologie. Travaux et Documents des Laboratoires de Géologie de*
843 *Lyon* 103, 3–317.
844
845 Dell'Unto, N., Landeschi, G., 2022. *Archaeological 3D GIS*, 1st ed. Routledge, London.
846 <https://doi.org/10.4324/9781003034131>
847
848 Dibble, H.L., Chase, P.G., McPherron, S.P., Tuffreau, A., 1997. Testing the Reality of a
849 “Living Floor” with Archaeological Data. *Am. antiq.* 62, 629–651.
850 <https://doi.org/10.2307/281882>
851
852 Ducke, B., 2012. Natives of a connected world: free and open source software in
853 archaeology. *World Archaeology* 44, 571–579.
854 <https://doi.org/10.1080/00438243.2012.743259>
855
856 ESRI, 2016. Que sont les données raster ? [WWW Document]. ArcGIS Desktop. URL
857 [https://desktop.arcgis.com/fr/arcmap/10.3/manage-data/raster-and-images/what-is-raster-](https://desktop.arcgis.com/fr/arcmap/10.3/manage-data/raster-and-images/what-is-raster-data.htm)
858 [data.htm](https://desktop.arcgis.com/fr/arcmap/10.3/manage-data/raster-and-images/what-is-raster-data.htm) (accessed 8.28.21).
859
860 Gabucio, M.J., Bargalló, A., Saladié, P., Romagnoli, F., Chacón, M.G., Vallverdú, J.,
861 Vaquero, M., 2023. Using GIS and Geostatistical Techniques to Identify Neanderthal
862 Campsites at archaeological level Ob at Abric Romani. *Archaeol Anthropol Sci* 15, 24.
863 <https://doi.org/10.1007/s12520-023-01715-6>
864

865 Galanidou, N., 2000. Patterns in Caves: Foragers, Horticulturists, and the Use of Space.
866 *Journal of Anthropological Archaeology* 19, 243–275.
867 <https://doi.org/10.1006/jaar.1999.0362>
868

869 Getis, A., Ord, J.K., 1992. The Analysis of Spatial Association by Use of Distance
870 Statistics. *Geographical Analysis* 24, 189–206. [https://doi.org/10.1111/j.1538-](https://doi.org/10.1111/j.1538-4632.1992.tb00261.x)
871 [4632.1992.tb00261.x](https://doi.org/10.1111/j.1538-4632.1992.tb00261.x)
872

873 Giusti, D., Turloukis, V., Konidaris, GeorgeE., Thompson, N., Karkanis, P.,
874 Panagopoulou, E., Harvati, K., 2018. Beyond maps: Patterns of formation processes at the
875 Middle Pleistocene open-air site of Marathousa 1, Megalopolis basin, Greece. *Quaternary*
876 *International* 497, 137–153. <https://doi.org/10.1016/j.quaint.2018.01.041>
877

878 Guillemot, P., 2021. Analyse spatiale des niveaux 4.1 et 4.2 de l’Abri du Maras (Ardèche,
879 France), approche combinée : SIG et 3D. (M.Sc. Dissertation). Muséum national
880 d’Histoire naturelle.
881

882 Hardy, B.L., Moncel, M.-H., Daujeard, C., Fernandes, P., Béarez, P., Desclaux, E.,
883 Chacon Navarro, M.G., Puaud, S., Gallotti, R., 2013. Impossible Neanderthals? Making
884 string, throwing projectiles and catching small game during Marine Isotope Stage 4 (Abri
885 du Maras, France). *Quaternary Science Reviews* 82, 23–40.
886 <https://doi.org/10.1016/j.quascirev.2013.09.028>
887

888 Hardy, B.L., Moncel, M.-H., Kerfant, C., Lebon, M., Bellot-Gurlet, L., Mélard, N., 2020.
889 Direct evidence of Neanderthal fibre technology and its cognitive and behavioral
890 implications. *Scientific Reports* 10, 4889. <https://doi.org/10.1038/s41598-020-61839-w>
891

892 Henry, D., 2012. The palimpsest problem, hearth pattern analysis, and Middle Paleolithic
893 site structure. *Quaternary International* 247, 246–266.
894 <https://doi.org/10.1016/j.quaint.2010.10.013>
895

896 Henry, D.O., Hietala, H.J., Rosen, A.M., Demidenko, Y.E., Usik, V.I., Armagan, T.L.,
897 2004. Human Behavioral Organization in the Middle Paleolithic: Were Neanderthals
898 Different? *American Anthropologist* 106, 17–31. <https://doi.org/10.1525/aa.2004.106.1.17>
899

900 Howey, M.C.L., Brouwer Burg, M., 2017. Assessing the state of archaeological GIS
901 research: Unbinding analyses of past landscapes. *Journal of Archaeological Science* 84, 1–
902 9. <https://doi.org/10.1016/j.jas.2017.05.002>
903

904 Ince, D.C., Hatton, L., Graham-Cumming, J., 2012. The case for open computer
905 programs. *Nature* 482, 485–488. <https://doi.org/10.1038/nature10836>
906

907 Jaillet, S., Sadier, B., Perazio, G., Delannoy, J.-J., 2014. Une brève histoire de la 3D en
908 grotte. *Karstologia* 63, 3–20.
909

910 Machado, J., Hernández, C.M., Mallol, C., Galván, B., 2013. Lithic production, site
911 formation and Middle Palaeolithic palimpsest analysis: in search of human occupation
912 episodes at Abric del Pastor Stratigraphic Unit IV (Alicante, Spain). *Journal of*
913 *Archaeological Science* 40, 2254–2273. <https://doi.org/10.1016/j.jas.2013.01.002>
914

- 915 Machado, J., Mayor, A., Hernández, C.M., Galván, B., 2019. Lithic refitting and the
916 analysis of Middle Palaeolithic settlement dynamics: a high-temporal resolution example
917 from El Pastor rock shelter (Eastern Iberia). *Archaeol Anthropol Sci* 11, 4539–4554.
918 <https://doi.org/10.1007/s12520-019-00859-8>
919
- 920 Malinsky-Buller, A., Hovers, E., Marder, O., 2011. Making time: ‘Living floors’,
921 ‘palimpsests’ and site formation processes – A perspective from the open-air Lower
922 Paleolithic site of Revadim Quarry, Israel. *Journal of Anthropological Archaeology* 30,
923 89–101. <https://doi.org/10.1016/j.jaa.2010.11.002>
924
- 925 Mallol, C., Hernández, C., 2016. Advances in palimpsest dissection. *Quaternary*
926 *International* 417, 1–2. <https://doi.org/10.1016/j.quaint.2016.09.021>
927
- 928 Marín, J., Daujeard, C., Saladié, P., Rodríguez-Hidalgo, A., Vettese, D., Rivals, F.,
929 Boulbes, N., Crégut-Bonnoure, E., Lateur, N., Gallotti, R., Arbez, L., Puaud, S., Moncel,
930 M.-H., 2020. Neanderthal faunal exploitation and settlement dynamics at the Abri du
931 Maras, level 5 (south-eastern France). *Quaternary Science Reviews* 243, 106472.
932 <https://doi.org/10.1016/j.quascirev.2020.106472>
933
- 934 McCoy, M.D., Ladefoged, T.N., 2009. New Developments in the Use of Spatial
935 Technology in Archaeology. *J Archaeol Res* 17, 263–295. [https://doi.org/10.1007/s10814-](https://doi.org/10.1007/s10814-009-9030-1)
936 [009-9030-1](https://doi.org/10.1007/s10814-009-9030-1)
937
- 938 Mellars, P., 1996. *The Neanderthal Legacy: An Archaeological Perspective from Western*
939 *Europe*. Princeton University Press.
940
- 941 Moncel, M.-H., Allué, E., Bailon, S., Barshay-Szmidt, C., Béarez, P., Crégut, É.,
942 Daujeard, C., Desclaux, E., Debard, É., Lartigot-Campin, A.-S., Puaud, S., Roger, T.,
943 2015. Evaluating the integrity of palaeoenvironmental and archaeological records in MIS
944 5 to 3 karst sequences from southeastern France. *Quaternary International* 378, 22–39.
945 <https://doi.org/10.1016/j.quaint.2013.12.009>
946
- 947 Moncel, M.-H., Chacón, M.G., La Porta, A., Fernandes, P., Hardy, B., Gallotti, R., 2014.
948 Fragmented reduction processes: Middle Palaeolithic technical behaviour in the Abri du
949 Maras shelter, southeastern France. *Quaternary International* 350, 180–204.
950 <https://doi.org/10.1016/j.quaint.2014.05.013>
951
- 952 Moncel, M.-H., Chacón, M.G., Vettese, D., Courty, M.-A., Daujeard, C., Eixea, A.,
953 Fernandes, P., Allué, E., Hardy, B., Rivals, F., Béarez, P., Gallotti, R., Puaud, S., 2021.
954 Late Neanderthal short-term and specialized occupations at the Abri du Maras (South-East
955 France, level 4.1, MIS 3). *Archaeol Anthropol Sci* 13, 45. [https://doi.org/10.1007/s12520-](https://doi.org/10.1007/s12520-021-01285-5)
956 [021-01285-5](https://doi.org/10.1007/s12520-021-01285-5)
957
- 958 Moncel, M.-H., Daujeard, C., Navarro, M., Vettese, D., Fernandes, P., Hardy, B., Puaud,
959 S., Richard, M., Allué, E., Béarez, P., Boulbes, N., Britton, K., Courty, M.-A., Crégut, E.,
960 Desclaux, E., Gallotti, R., Joannes-Boyau, R., Kerfant, C., Lateur, N., Falguères, C., 2018.
961 L’Abri du Maras. À Saint-Martin d’Ardèche, des habitats néandertaliens du début du
962 dernier glaciaire 35, 3–11.
963
- 964 Moncel, M.-H., Gaillard, C., Patou-Mathis, M., 1994. L’abri du Maras (Ardèche) : une

965 nouvelle campagne de fouilles dans un site Paléolithique moyen (1993). *Bulletin de la*
966 *Société préhistorique française* 91, 363–368. <https://doi.org/10.3406/bspf.1994.9786>
967

968 Mora Torcal, R., Roy Sunyer, M., Martínez-Moreno, J., Benito-Calvo, A., Samper Carro,
969 S., 2020. Inside the Palimpsest: Identifying Short Occupations in the 497D Level of Cova
970 Gran (Iberia), in: Cascalheira, J., Picin, A. (Eds.), *Short-Term Occupations in Paleolithic*
971 *Archaeology, Interdisciplinary Contributions to Archaeology*. Springer International
972 Publishing, Cham, pp. 39–69. https://doi.org/10.1007/978-3-030-27403-0_3
973

974 Morin, A., Urban, J., Adams, P.D., Foster, I., Sali, A., Baker, D., Sliz, P., 2012. Shining
975 Light into Black Boxes. *Science* 336, 159–160. <https://doi.org/10.1126/science.1218263>
976

977 Neruda, P., 2017. GIS analysis of the spatial distribution of Middle Palaeolithic artefacts
978 in Kůlna Cave (Czech Republic). *Quaternary International* 435, 58–76.
979 <https://doi.org/10.1016/j.quaint.2015.10.028>
980

981 Ord, J.K., Getis, A., 1995. Local Spatial Autocorrelation Statistics: Distributional Issues
982 and an Application. *Geographical Analysis* 27, 286–306. [https://doi.org/10.1111/j.1538-](https://doi.org/10.1111/j.1538-4632.1995.tb00912.x)
983 [4632.1995.tb00912.x](https://doi.org/10.1111/j.1538-4632.1995.tb00912.x)
984

985 Orengo, H., 2015. Open source GIS and geospatial software in archaeology: towards their
986 integration into everyday archaeological practice, in: Wilson, A.T., Edwards, B. (Eds.),
987 *Open Source Archaeology: Ethics and Practice*. De Gruyter Open, Warsaw Berlin, pp. 64–
988 82.
989

990 Oron, M., Goren-Inbar, N., 2014. Mousterian intra-site spatial patterning at Quneitra,
991 Golan Heights. *Quaternary International* 331, 186–202.
992 <https://doi.org/10.1016/j.quaint.2013.04.013>
993

994 Oxoli, D., Molinari, M., Brovelli, M., 2018. Hotspot Analysis, an open source GIS tool
995 for exploratory spatial data analysis: application to the study of soil consumption in Italy.
996 *Rendiconti Online della Società Geologica Italiana* 46, 82–87.
997 <https://doi.org/10.3301/ROL.2018.56>
998

999 Oxoli, D., Prestifilippo, G., Bertocchi, D., Zurbarán, M., 2017. Enabling spatial
1000 autocorrelation mapping in QGIS: The hotspot analysis plugin. *Geoinformatica Ambientale*
1001 *e Mineraria* 151, 45–50.
1002

1003 Oxoli, D., Zurbarán, M.A., Shaji, S., Muthusamy, A.K., 2016. Hotspot analysis: a first
1004 prototype Python plugin enabling exploratory spatial data analysis into QGIS. *PeerJ*
1005 *Preprints* 4, e2204v4. <https://doi.org/10.7287/peerj.preprints.2204v4>
1006

1007 Petraglia, M.D., Potts, R., 1994. Water Flow and the Formation of Early Pleistocene
1008 Artifact Sites in Olduvai Gorge, Tanzania. *Journal of Anthropological Archaeology* 13,
1009 228–254. <https://doi.org/10.1006/jaar.1994.1014>
1010

1011 Pettitt, P.B., 1997. High resolution Neanderthals? Interpreting middle palaeolithic intrasite
1012 spatial data. *World Archaeology* 29, 208–224.
1013 <https://doi.org/10.1080/00438243.1997.9980374>
1014

1015 Picin, A., Cascalheira, J., 2020. Introduction to Short-Term Occupations in Palaeolithic
1016 Archaeology, in: Cascalheira, J., Picin, A. (Eds.), Short-Term Occupations in Paleolithic
1017 Archaeology, Interdisciplinary Contributions to Archaeology. Springer International
1018 Publishing, Cham, pp. 1–15. https://doi.org/10.1007/978-3-030-27403-0_1
1019

1020 Puaud, S., Nowak, M., Pont, S., Moncel, M.-H., 2015. Minéraux volcaniques et alpins à
1021 l’abri du Maras (Ardèche, France) : témoins de vents catabatiques dans la vallée du Rhône
1022 au Pléistocène supérieur. *Comptes Rendus Palevol* 14, 331–341.
1023 <https://doi.org/10.1016/j.crpv.2015.02.007>
1024

1025 QGIS.org, 2021. QGIS Geographic Information System.
1026

1027 Reeves, J.S., McPherron, S.P., Aldeias, V., Dibble, H.L., Goldberg, P., Sandgathe, D.,
1028 Turq, A., 2019. Measuring spatial structure in time-averaged deposits insights from Roc
1029 de Marsal, France. *Archaeol Anthropol Sci* 11, 5743–5762.
1030 <https://doi.org/10.1007/s12520-019-00871-y>
1031

1032 Richard, M., Falguères, C., Pons-Branchu, E., Bahain, J.-J., Voinchet, P., Lebon, M.,
1033 Valladas, H., Dolo, J.-M., Puaud, S., Rué, M., Daujeard, C., Moncel, M.-H., Raynal, J.-P.,
1034 2015. Contribution of ESR/U-series dating to the chronology of late Middle Palaeolithic
1035 sites in the middle Rhône valley, southeastern France. *Quaternary Geochronology, LED14*
1036 *Proceedings* 30, 529–534. <https://doi.org/10.1016/j.quageo.2015.06.002>
1037

1038 Richard, M., Pons-Branchu, E., Genuite, K., Jaillet, S., Joannes-Boyau, R., Wang, N.,
1039 Genty, D., Cheng, H., Price, G.J., Pierre, M., Dapoigny, A., Falguères, C., Tombret, O.,
1040 Voinchet, P., Bahain, J.-J., Moncel, M.-H., 2021. Timing of Neanderthal occupations in
1041 the southeastern margins of the Massif Central (France): A multi-method approach.
1042 *Quaternary Science Reviews* 273, 107241.
1043 <https://doi.org/10.1016/j.quascirev.2021.107241>
1044

1045 Richards-Rissetto, H., 2017. What can GIS + 3D mean for landscape archaeology?
1046 *Journal of Archaeological Science* 84, 10–21. <https://doi.org/10.1016/j.jas.2017.05.005>
1047

1048 Romagnoli, F., Vaquero, M., 2016. Quantitative stone tools intra-site points and
1049 orientation patterns of a Middle Palaeolithic living floor: A GIS multi-scalar spatial and
1050 temporal approach. *Quartär* 63, 47–60. https://doi.org/10.7485/QU63_3
1051

1052 Sánchez-Romero, L., Benito-Calvo, A., Marín-Arroyo, A.B., Agudo-Pérez, L.,
1053 Karampaglidis, T., Rios-Garaizar, J., 2020. New insights for understanding spatial
1054 patterning and formation processes of the Neanderthal occupation in the Amalda I cave
1055 (Gipuzkoa, Spain). *Sci Rep* 10, 8733. <https://doi.org/10.1038/s41598-020-65364-8>
1056

1057 Sánchez-Romero, L., Benito-Calvo, A., Pérez-González, A., Santonja, M., 2016.
1058 Assessment of Accumulation Processes at the Middle Pleistocene Site of Ambrona (Soria,
1059 Spain). Density and Orientation Patterns in Spatial Datasets Derived from Excavations
1060 Conducted from the 1960s to the Present. *PLoS ONE* 11, e0167595.
1061 <https://doi.org/10.1371/journal.pone.0167595>
1062

1063 Sánchez-Romero, L., Benito-Calvo, A., Rios-Garaizar, J., 2021. Defining and
1064 Characterising Clusters in Palaeolithic Sites: a Review of Methods and Constraints. *J*

1065 Archaeol Method Theory. <https://doi.org/10.1007/s10816-021-09524-8>
1066
1067 Sañudo, P., Vallverdú-Poch, J., Canals, A., 2012. Spatial Patterns in Level J, in: Carbonell
1068 i Roura, E. (Ed.), High Resolution Archaeology and Neanderthal Behavior, Vertebrate
1069 Paleobiology and Paleoanthropology. Springer Netherlands, Dordrecht, pp. 47–76.
1070 https://doi.org/10.1007/978-94-007-3922-2_3
1071
1072 Spagnolo, V., Marciani, G., Aureli, D., Berna, F., Toniello, G., Astudillo, F., Boschin, F.,
1073 Boscato, P., Ronchitelli, A., 2019. Neanderthal activity and resting areas from
1074 stratigraphic unit 13 at the Middle Palaeolithic site of Oscurusciuto (Ginosa - Taranto,
1075 Southern Italy). *Quaternary Science Reviews* 217, 169–193.
1076 <https://doi.org/10.1016/j.quascirev.2018.06.024>
1077
1078 Spagnolo, V., Marciani, G., Aureli, D., Martini, I., Boscato, P., Boschin, F., Ronchitelli,
1079 A., 2020. Climbing the time to see Neanderthal behaviour’s continuity and discontinuity:
1080 SU 11 of the Oscurusciuto Rockshelter (Ginosa, Southern Italy). *Archaeol Anthropol Sci*
1081 12, 54. <https://doi.org/10.1007/s12520-019-00971-9>
1082
1083 Stavrova, T., Borel, A., Daujeard, C., Vettese, D., 2019. A GIS based approach to long
1084 bone breakage patterns derived from marrow extraction. *PLoS ONE* 14, e0216733.
1085 <https://doi.org/10.1371/journal.pone.0216733>
1086
1087 Vaquero, M., 2008. The history of stones: behavioural inferences and temporal resolution
1088 of an archaeological assemblage from the Middle Palaeolithic. *Journal of Archaeological*
1089 *Science* 35, 3178–3185. <https://doi.org/10.1016/j.jas.2008.07.006>
1090
1091 Vaquero, M., Chacón, M.G., García-Antón, M.D., Gómez de Soler, B., Martínez, K.,
1092 Cuartero, F., 2012. Time and space in the formation of lithic assemblages: The example of
1093 Abric Romaní Level J. *Quaternary International* 247, 162–181.
1094 <https://doi.org/10.1016/j.quaint.2010.12.015>
1095
1096 Vaquero, M., Fernández-Laso, M.C., Chacón, M.G., Romagnoli, F., Rosell, J., Sañudo, P.,
1097 2017. Moving things: Comparing lithic and bone refits from a Middle Paleolithic site.
1098 *Journal of Anthropological Archaeology* 48, 262–280.
1099 <https://doi.org/10.1016/j.jaa.2017.09.001>
1100
1101 Vaquero, M., Pastó, I., 2001. The Definition of Spatial Units in Middle Palaeolithic Sites:
1102 The Hearth-Related Assemblages. *Journal of Archaeological Science* 28, 1209–1220.
1103 <https://doi.org/10.1006/jasc.2001.0656>
1104
1105 Vaquero, M., Romagnoli, F., Bargalló, A., Chacón, M.G., Gómez de Soler, B., Picin, A.,
1106 Carbonell, E., 2019. Lithic refitting and intrasite artifact transport: a view from the Middle
1107 Paleolithic. *Archaeol Anthropol Sci* 11, 4491–4513. <https://doi.org/10.1007/s12520-019-00832-5>
1108
1109
1110 Vaquero, M., Vallverdú, J., Rosell, J., Pastó, I., Allué, E., 2001. Neandertal Behavior at
1111 the Middle Palaeolithic Site of Abric Romaní, Capellades, Spain. *Journal of Field*
1112 *Archaeology* 28, 93–114. <https://doi.org/10.1179/jfa.2001.28.1-2.93>
1113
1114 Vettese, D., Borel, A., Blasco, R., Chevillard, L., Stavrova, T., Thun Hohenstein, U.,

1115 Arzarello, M., Moncel, M.-H., Daujeard, C., 2022. New evidence of Neandertal butchery
1116 traditions through the marrow extraction in southwestern Europe (MIS 5–3). PLoS ONE
1117 17, e0271816. <https://doi.org/10.1371/journal.pone.0271816>
1118

1119 Vettese, D., Daujeard, C., Blasco, R., Borel, A., Caceres, I., Moncel, M.H., 2017.
1120 Neandertal long bone breakage process: Standardized or random patterns? The example of
1121 Abri du Maras (Southeastern France, MIS 3). *Journal of Archaeological Science: Reports*
1122 13, 151–163. <https://doi.org/10.1016/j.jasrep.2017.03.029>
1123

1124 Vignes, M.-P., 2021. Approche multidisciplinaire des stratégies de subsistance des
1125 Néandertaliens à l'Abri du Maras (Ardèche): Archéozoologie, taphonomie et analyse
1126 spatiale de la grande faune du niveau 4.2 (MIS 3). (M.Sc. Dissertation). Muséum national
1127 d'Histoire naturelle.
1128

1129 Westoby, M.J., Brasington, J., Glasser, N.F., Hambrey, M.J., Reynolds, J.M., 2012.
1130 'Structure-from-Motion' photogrammetry: A low-cost, effective tool for geoscience
1131 applications. *Geomorphology* 179, 300–314.
1132 <https://doi.org/10.1016/j.geomorph.2012.08.021>
1133

1134 Whitley, T.G., 2017. Geospatial analysis as experimental archaeology. *Journal of*
1135 *Archaeological Science* 84, 103–114. <https://doi.org/10.1016/j.jas.2017.05.008>
1136
1137

1138 **Figure caption list** 1139

1140 **Figure 1.** Methodology used for palaeotopographic rendering and analysis of levels 4.1 and
1141 4.2.
1142

1143 **Figure 2.** Spatial patterns of lithics, bones and fire-related artefacts from Maras level 4.1.
1144 Hotspot analysis applied to lithic artefacts (A); hotspot analysis applied to faunal remains (B);
1145 spatial analysis of fire-related artefacts: kernel density of burnt lithics, hotspot analysis of
1146 charcoal remains and ash lenses scattering (C).
1147

1148 **Figure 3.** Hotspot analysis of the two RMUs with the most pieces: hotspot analysis of the
1149 RMU flint-13 (A), hotspot analysis of the RMU quartz-5 (B) from Maras level 4.1.
1150

1151 **Figure 4.** Kernel density of tool kits from Maras level 4.1.
1152

1153 **Figure 5.** Hotspot analysis of cortical flakes from Maras level 4.1.
1154

1155 **Figure 6.** Hotspot analysis of lithic tools from Maras level 4.1.
1156

1157 **Figure 7.** Hotspot analysis according to the length of lithic artefacts from Maras level 4.1.
1158

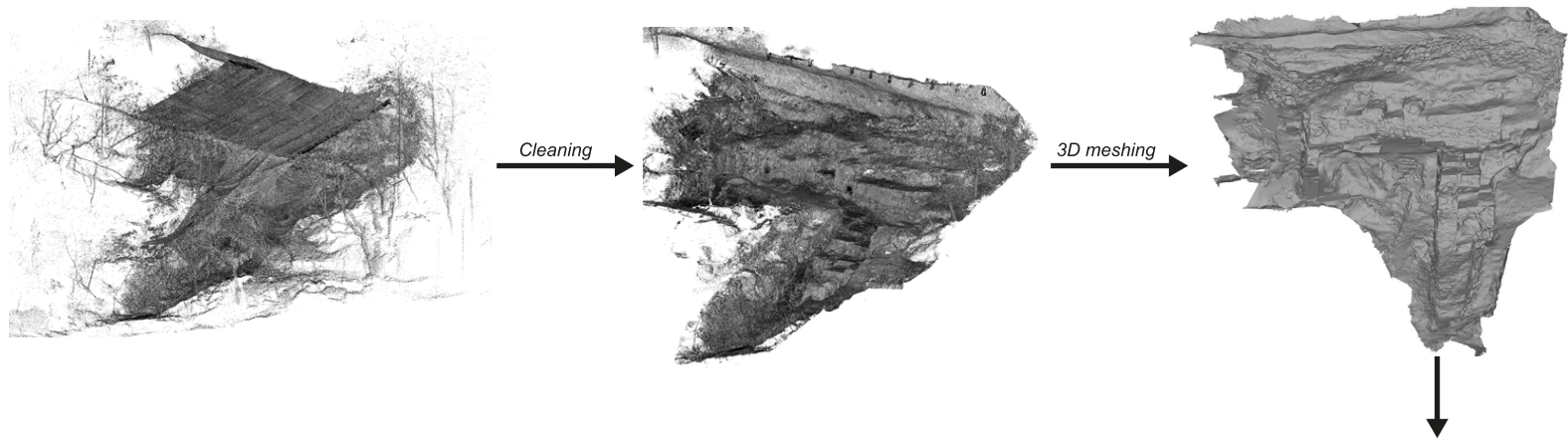
1159 **Figure 8.** Spatial patterns of lithics, bones and fire-related artefacts from Maras level 4.2.
1160 Hotspot analysis applied to lithic artefacts (A); hotspot analysis applied to faunal remains (B);
1161 spatial analysis of fire-related artefacts: kernel density of burnt lithics, hotspot analysis of
1162 charcoal remains and ash lenses scattering (C).
1163

1164 **Figure 9.** Hotspot analysis of cortical flakes from Maras level 4.2.

1165
1166 **Figure 10.** Hotspot analysis of lithic tools from Maras level 4.2.
1167
1168 **Figure 11.** Hotspot analysis of cores from Maras level 4.2.
1169
1170 **Figure 12.** Hotspot analysis according to the length of lithic artefacts from Maras level 4.2
1171 (dotted circles represent clusters in the disturbed areas of the site).
1172
1173 **Figure 13.** Palaeotopography of level 4.1: palaeosurface rendering of level 4.1 in the 3D mesh
1174 model of the Abri du Maras (A), DTM of the surface of level 4.1 with N-S and W-E
1175 palaeotopographic profiles.
1176
1177 **Figure 14.** Palaeotopography of level 4.2: palaeosurface rendering of level 4.2 within the 3D
1178 mesh model of the Abri du Maras (A), DTM of the surface of level 4.2 with N-S and W-E
1179 palaeotopographic profiles.
1180
1181 **Figure 15.** Spatial patterns identified from the spatial analysis of Maras level 4.1 (A) & level
1182 4.2 (B).

Figure 1

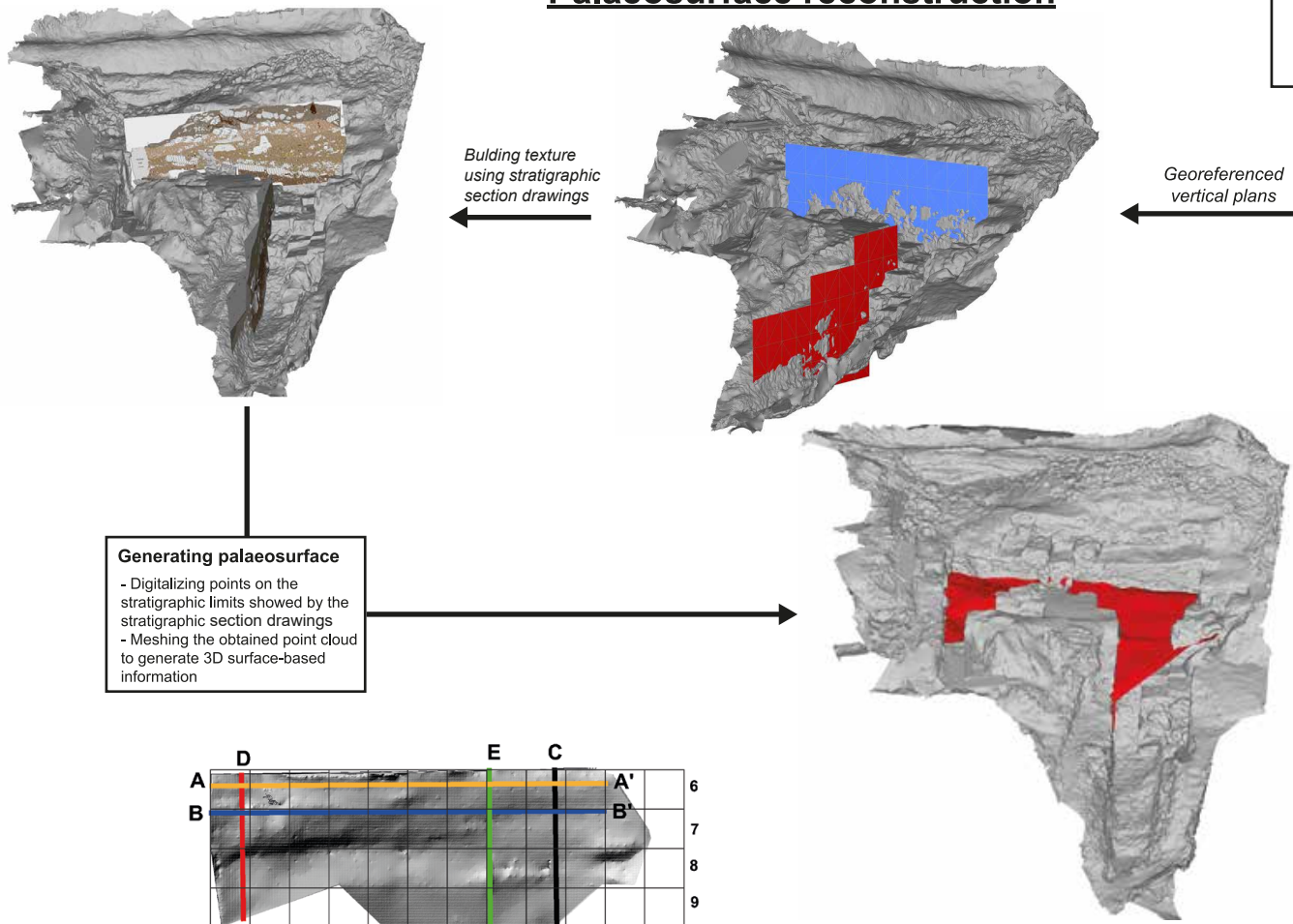
Preliminary processing on the 3D model



Modification of the coordinate system

- Rotation
- Translation in X, Y and Z coordinates

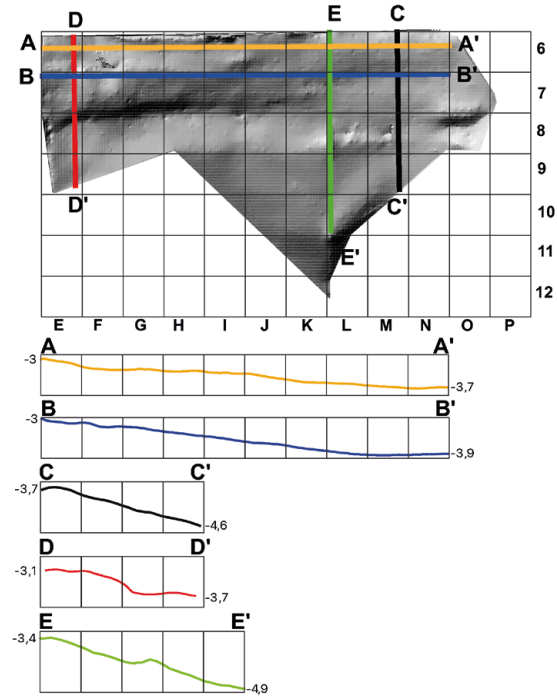
Palaeosurface reconstruction



Generating palaeosurface

- Digitalizing points on the stratigraphic limits showed by the stratigraphic section drawings
- Meshing the obtained point cloud to generate 3D surface-based information

Analysing palaeotopography in 2D



QGIS analysis

- Rasterising 3D surface into DTM
- Saving as TIF file
- Importing into QGIS
- Using profil tool

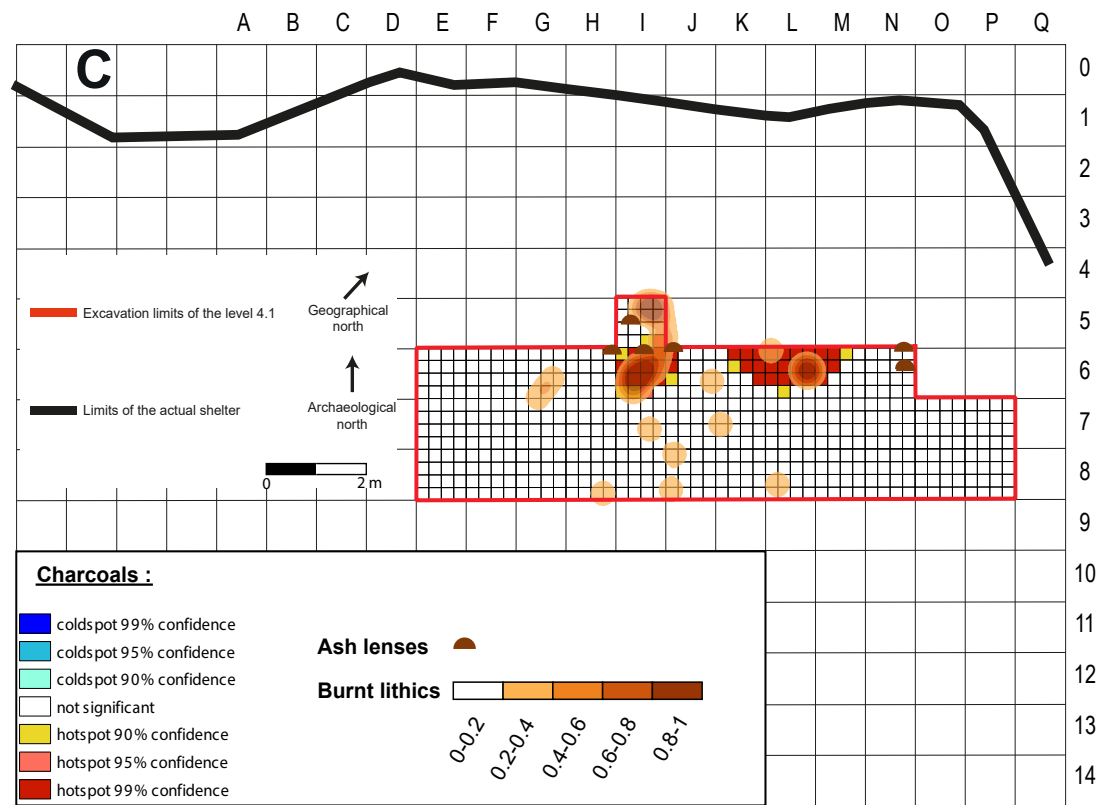
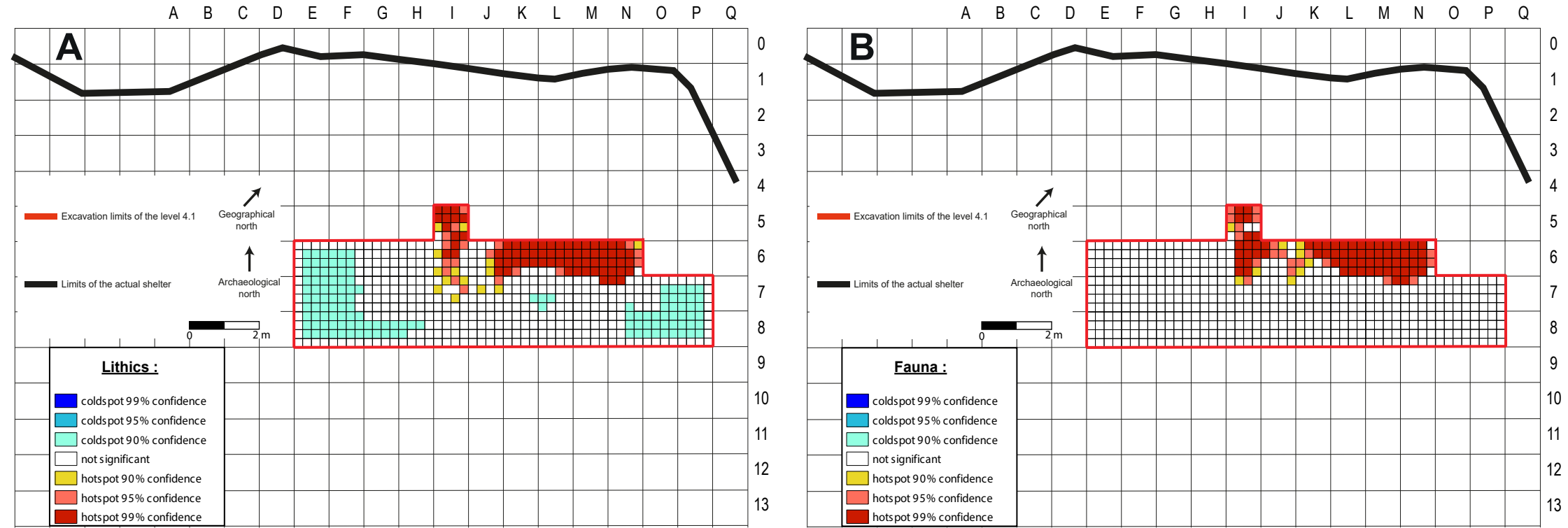
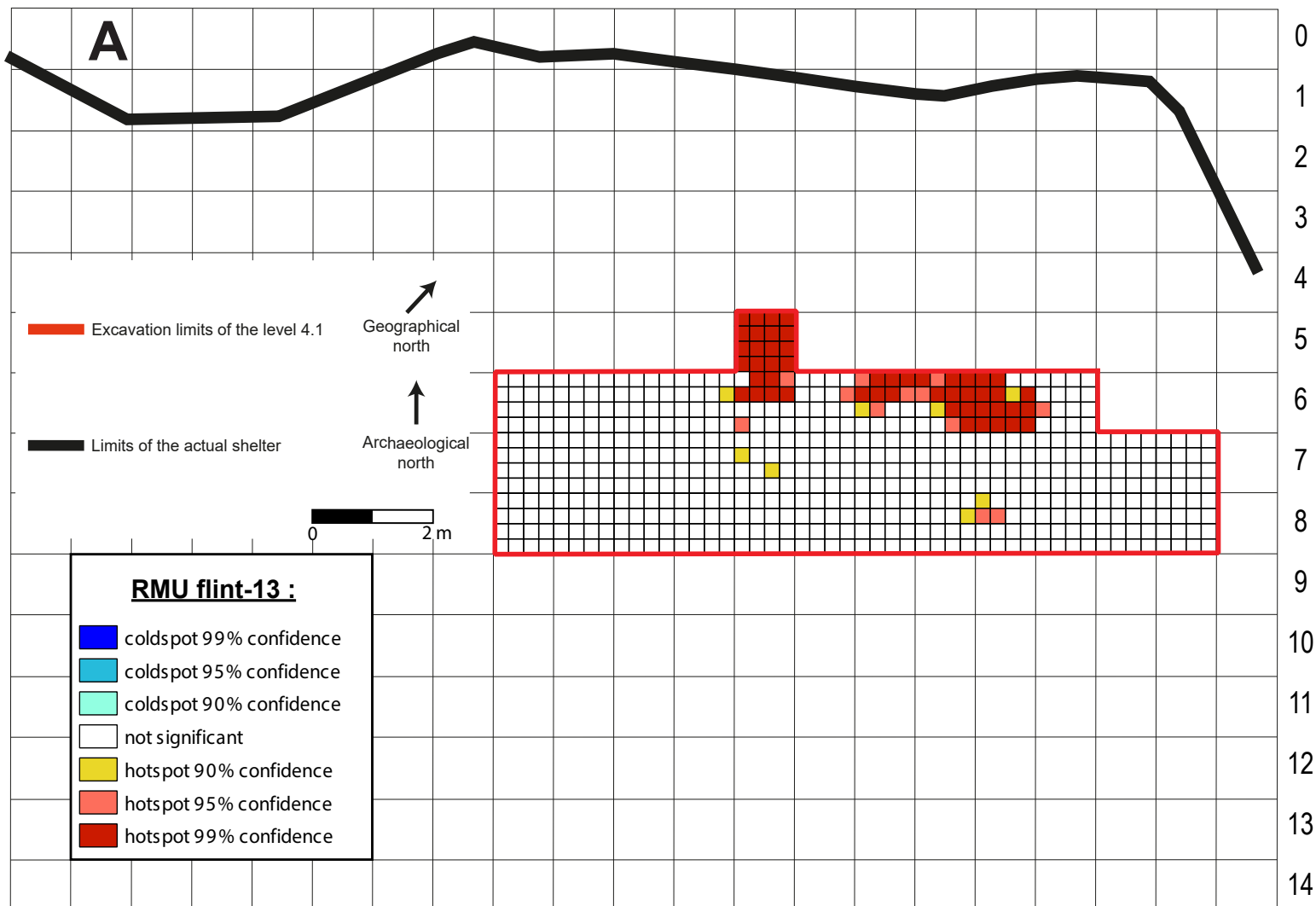


Figure 2

Figure 3

A B C D E F G H I J K L M N O P Q



A B C D E F G H I J K L M N O P Q

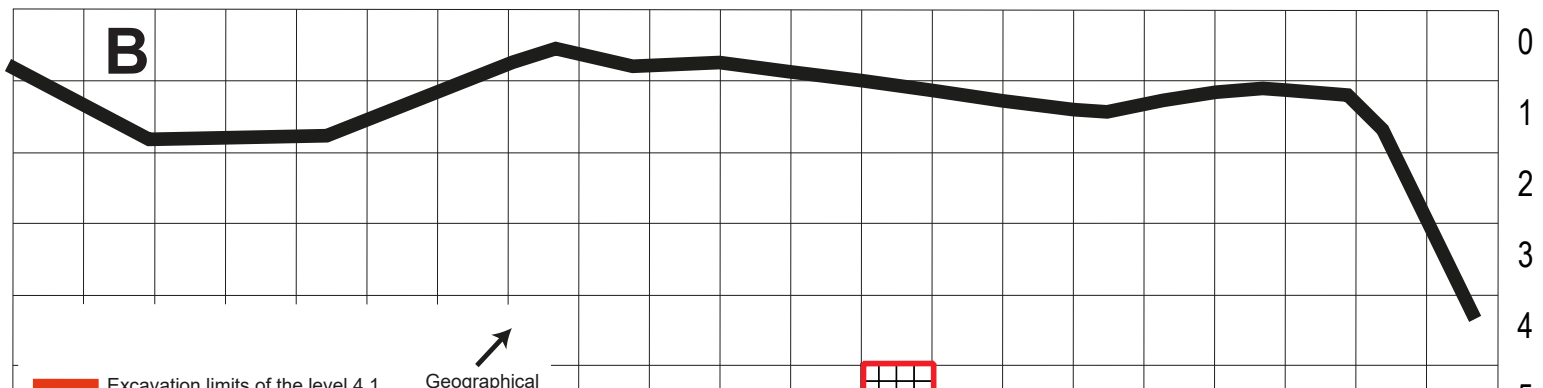


Figure 4

A B C D E F G H I J K L M N O P Q

0
1
2
3
4
5
6
7
8
9
10
11
12
13
14

Excavation limits of the level 4.1

Geographical north

Limits of the actual shelter

Archaeological north

0 2 m

Too kits



0-0.2
0.2-0.4
0.4-0.6
0.6-0.8
0.8-1

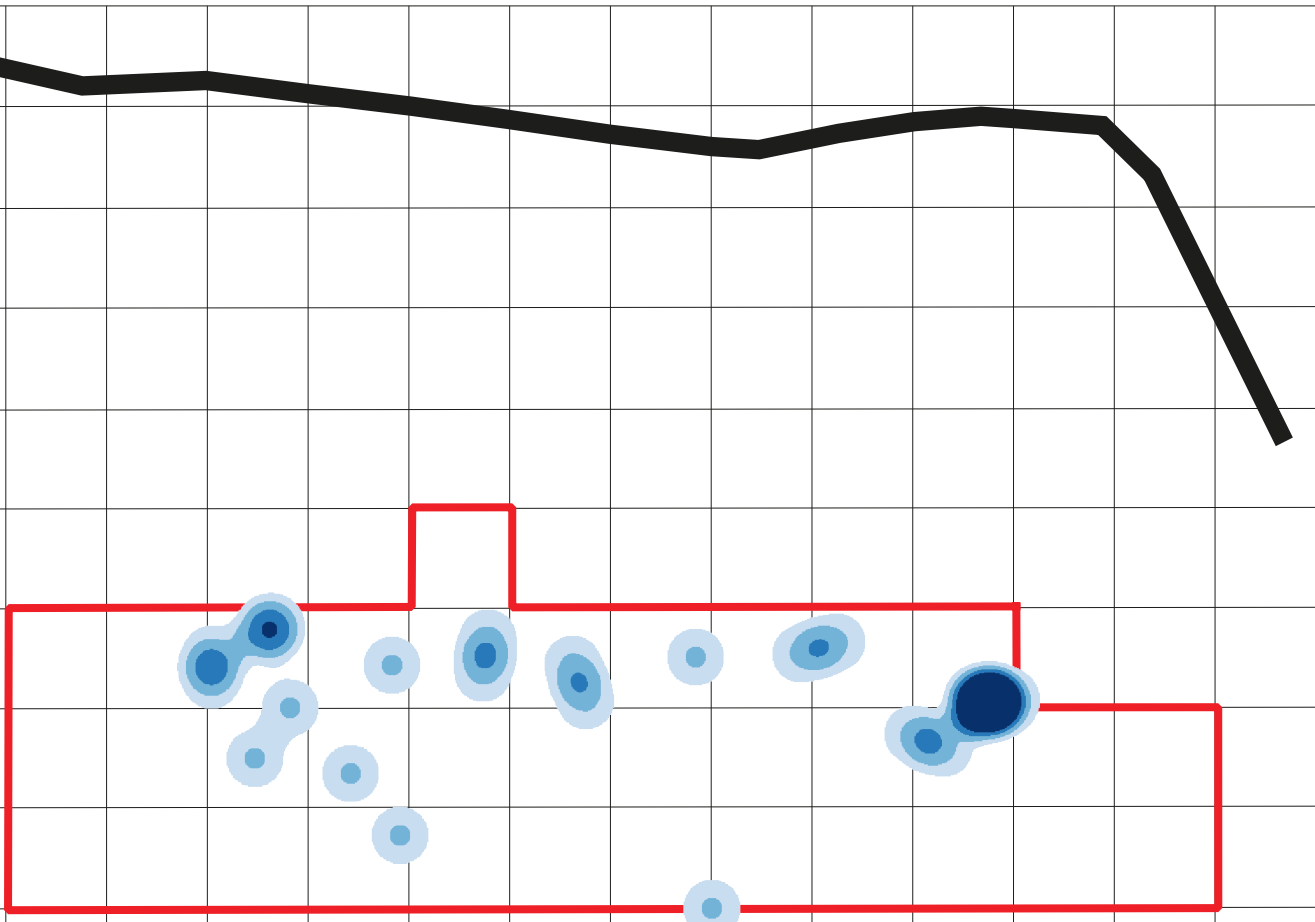


Figure 5

A B C D E F G H I J K L M N O P Q

0
1
2
3
4
5
6
7
8
9
10
11
12
13
14

Excavation limits of the level 4.1

Geographical north

Limits of the actual shelter

Archaeological north

0 2 m

Cortical flakes :

- coldspot 99% confidence
- coldspot 95% confidence
- coldspot 90% confidence
- not significant
- hotspot 90% confidence
- hotspot 95% confidence
- hotspot 99% confidence

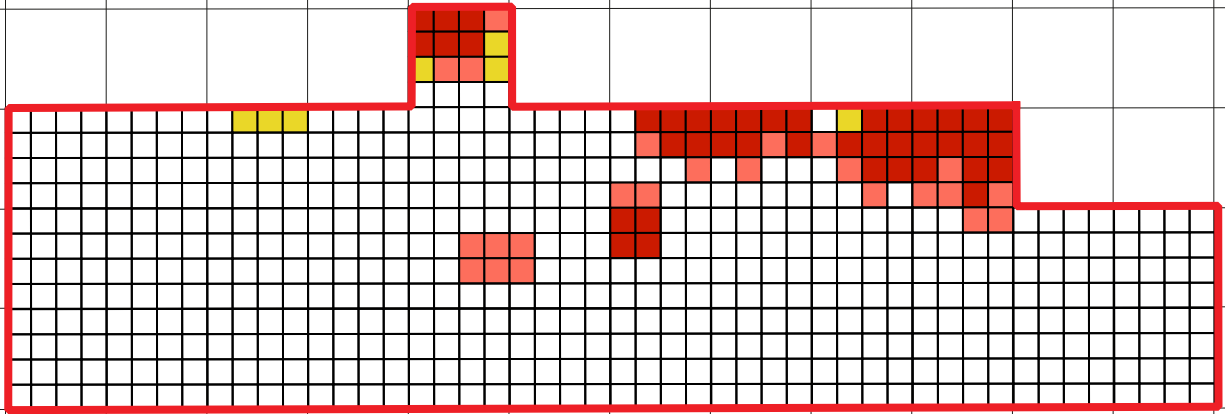
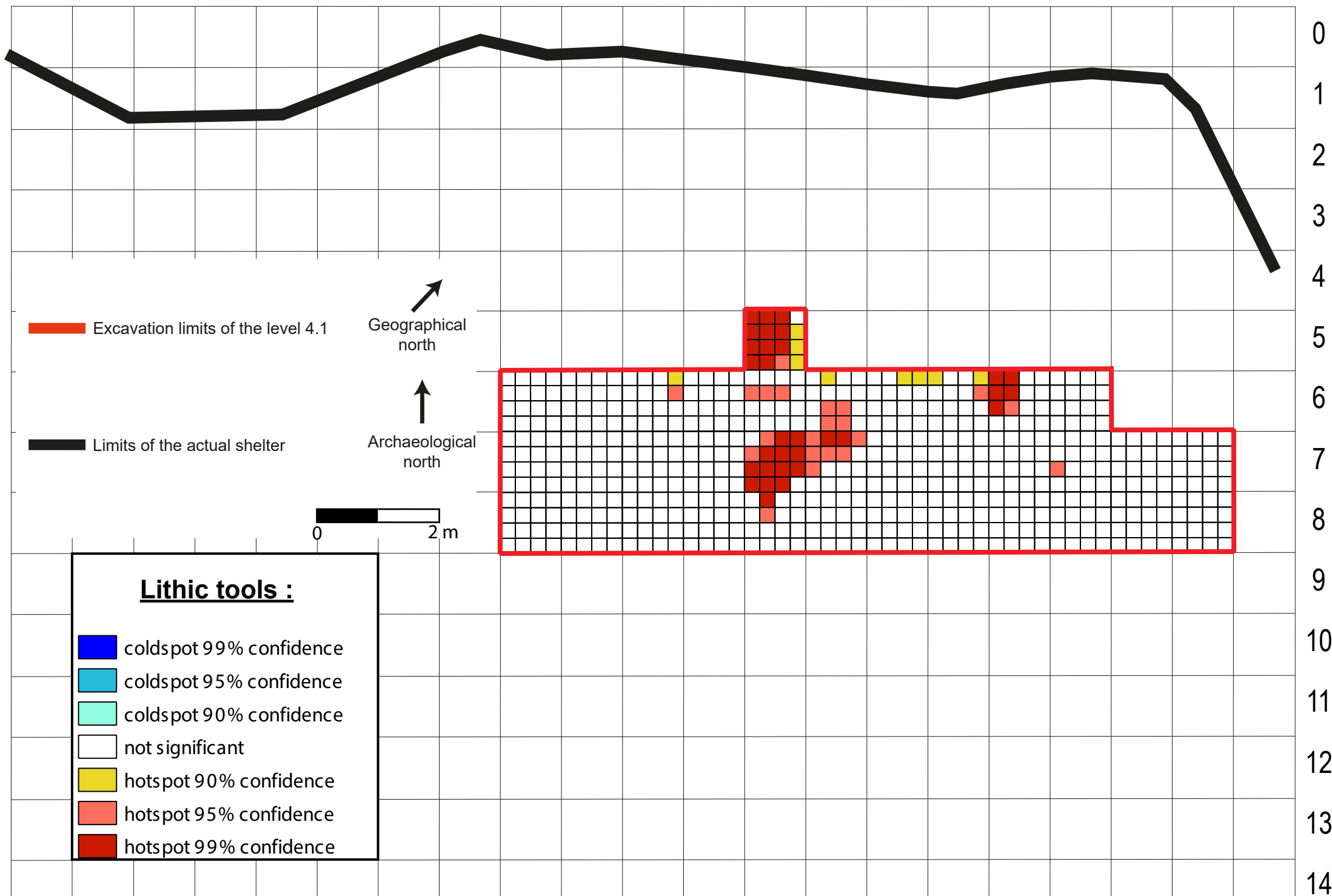


Figure 6

A B C D E F G H I J K L M N O P Q



Excavation limits of the level 4.1

Geographical north

Limits of the actual shelter

Archaeological north

0 2 m

Lithic tools :

- coldspot 99% confidence
- coldspot 95% confidence
- coldspot 90% confidence
- not significant
- hotspot 90% confidence
- hotspot 95% confidence
- hotspot 99% confidence

Figure 7

A B C D E F G H I J K L M N O P Q

0
1
2
3
4
5
6
7
8
9
10
11
12
13
14

Excavation limits of the level 4.1

Geographical north

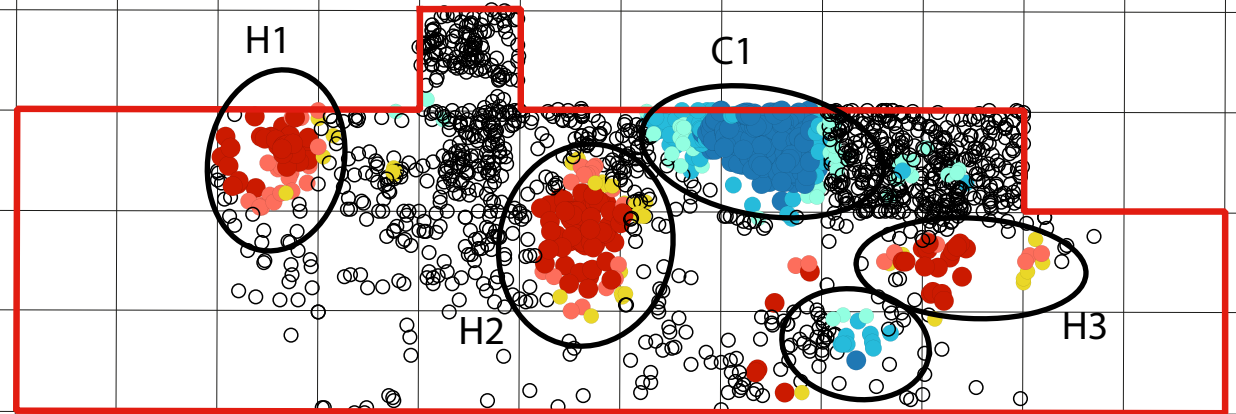
Limits of the actual shelter

Archaeological north

0 2 m

Length:

- coldspot 99% confidence
- coldspot 95% confidence
- coldspot 90% confidence
- not significant
- hotspot 90% confidence
- hotspot 95% confidence
- hotspot 99% confidence



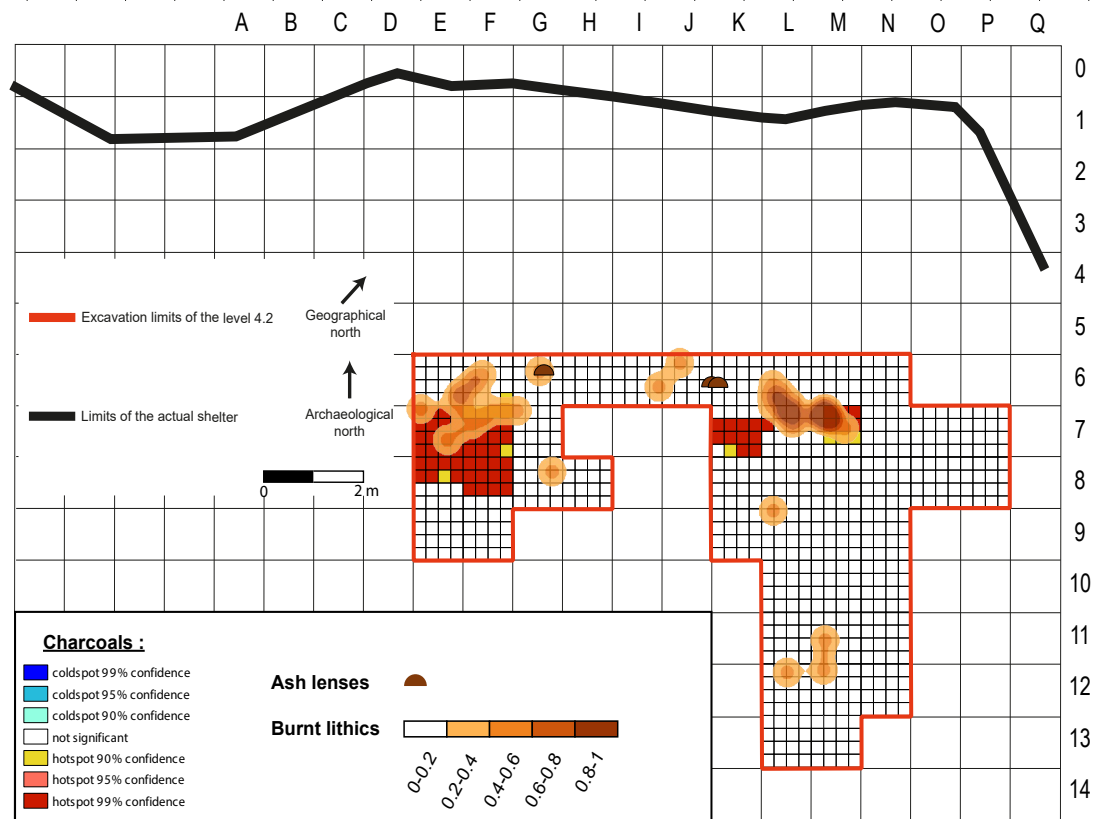
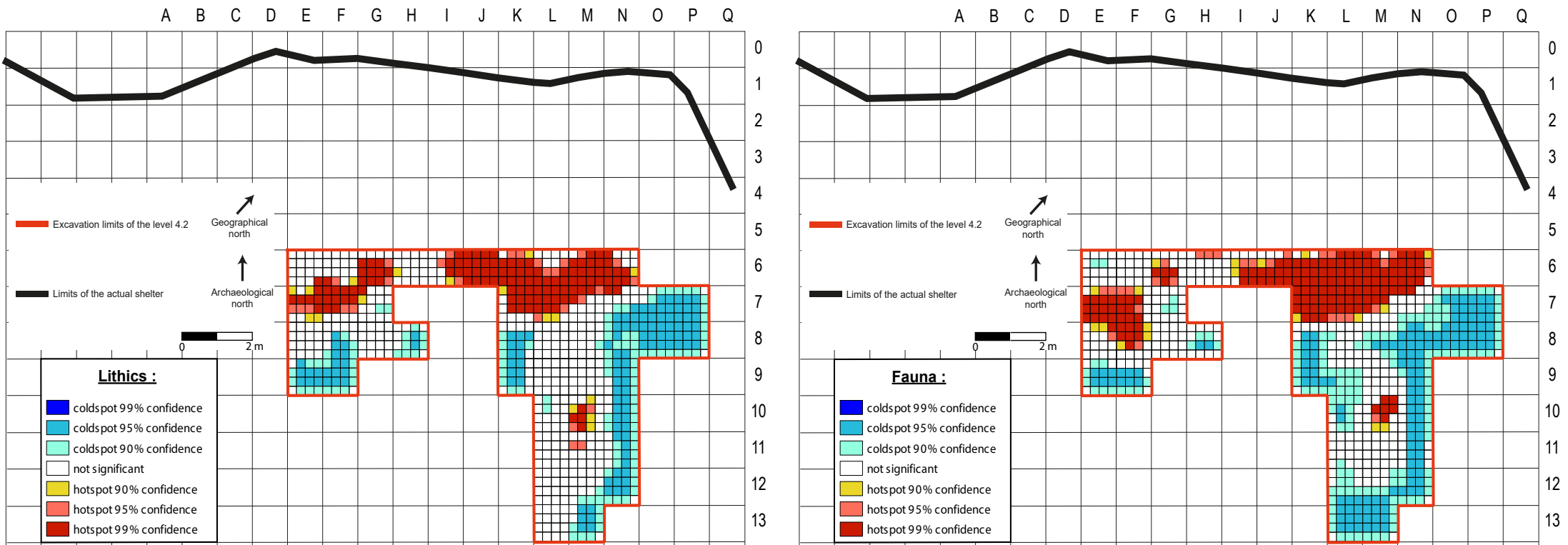


Figure 8

Figure 9

A B C D E F G H I J K L M N O P Q

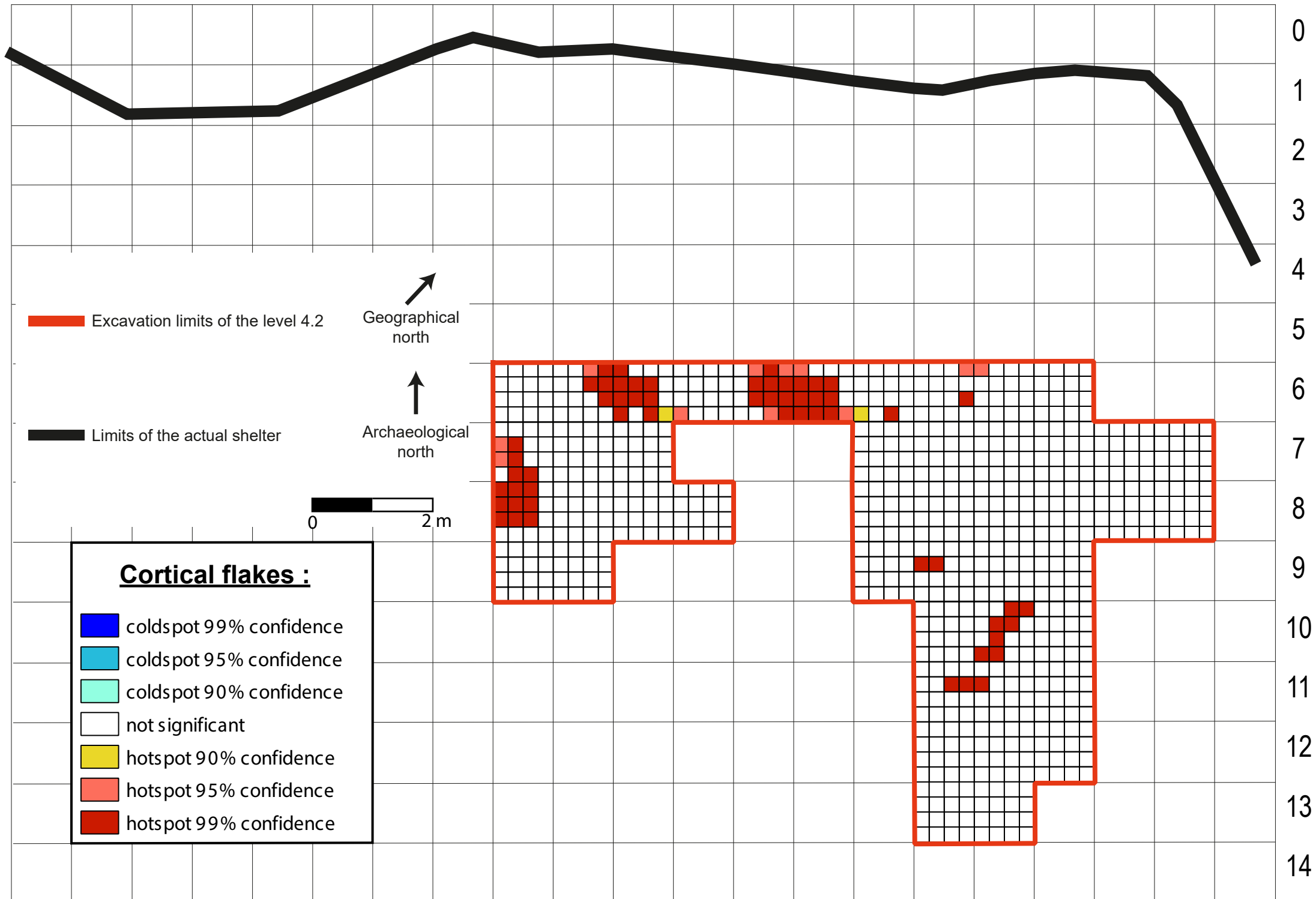


Figure 10

A B C D E F G H I J K L M N O P Q

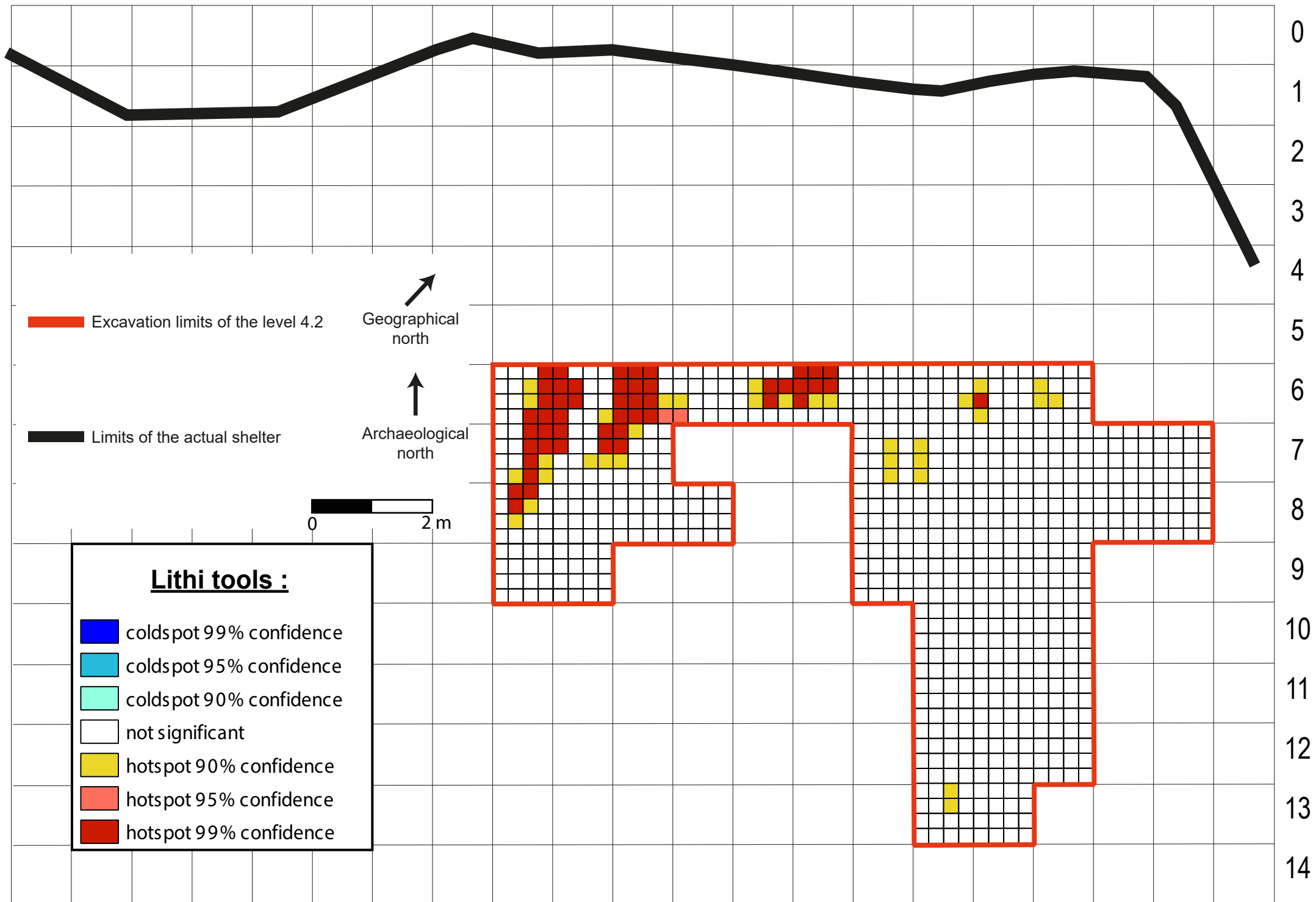


Figure 11

A B C D E F G H I J K L M N O P Q

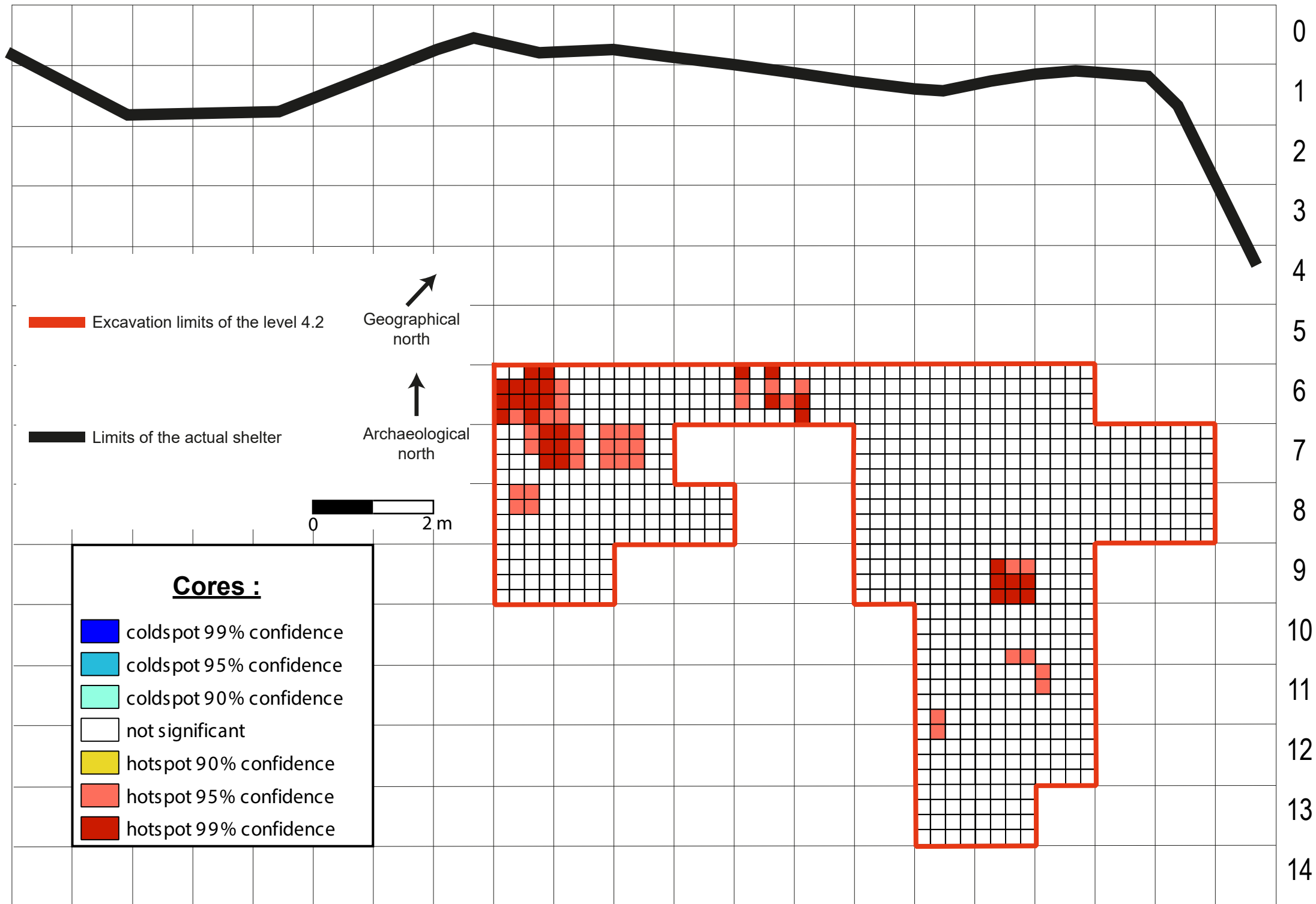
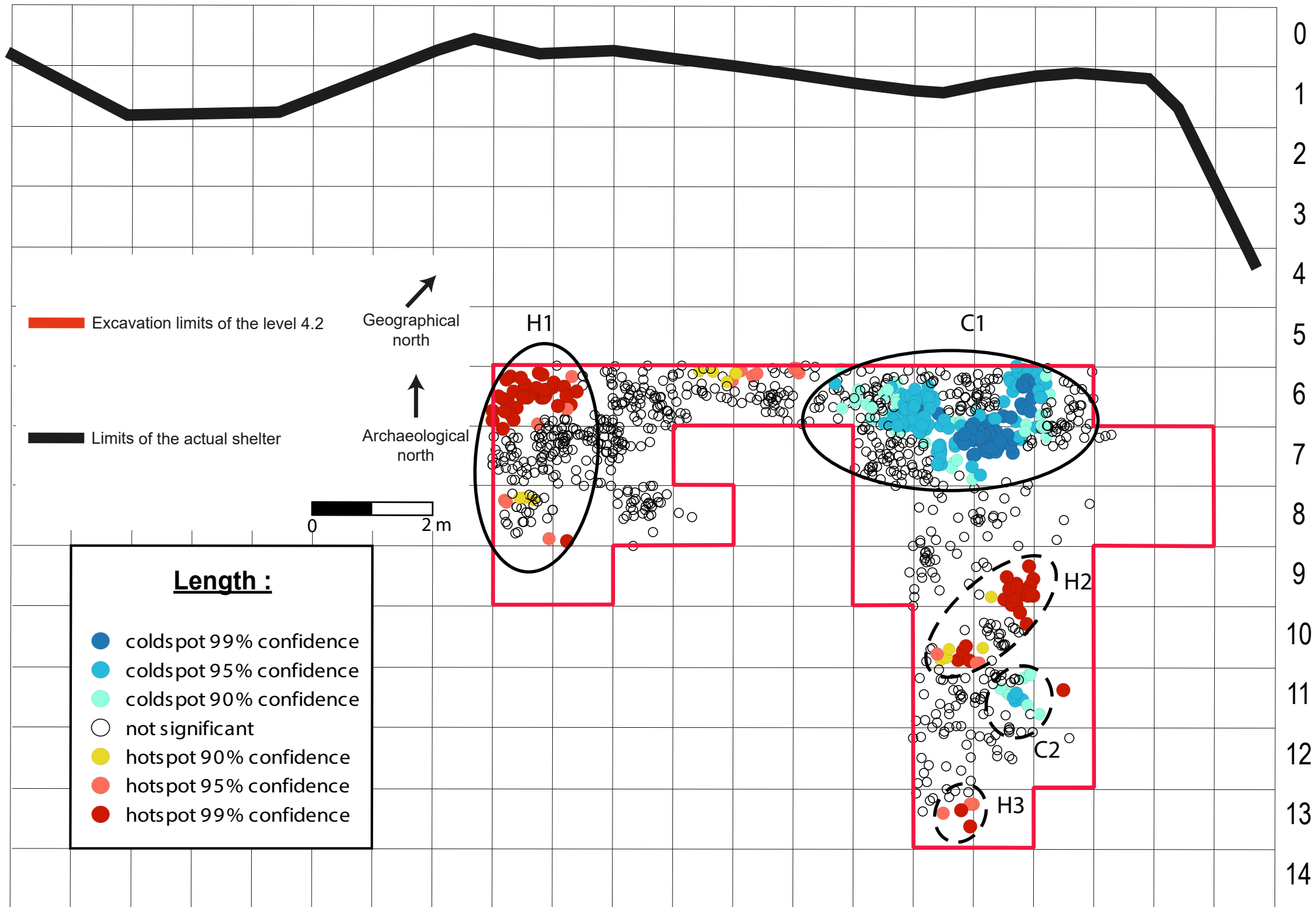


Figure 12

A B C D E F G H I J K L M N O P Q



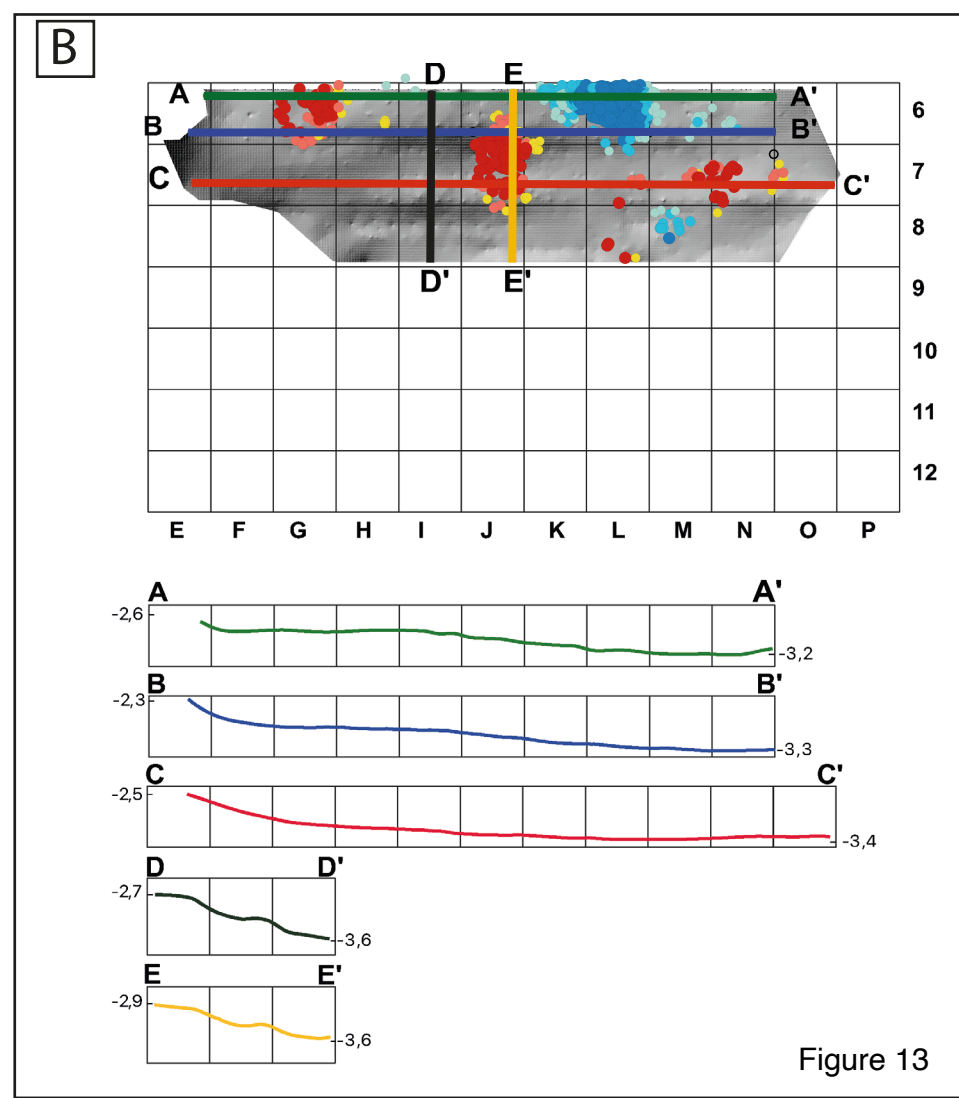
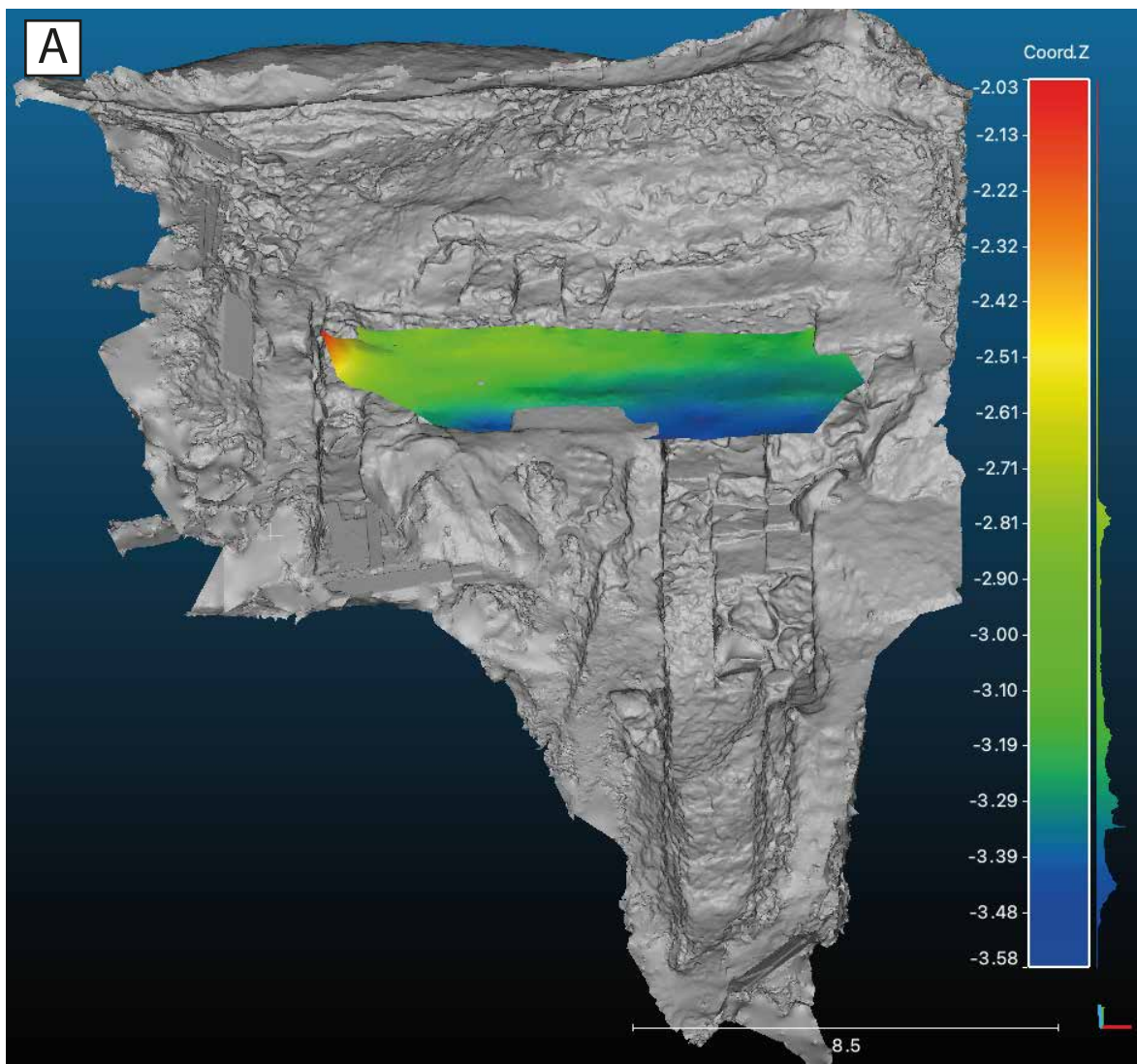


Figure 13

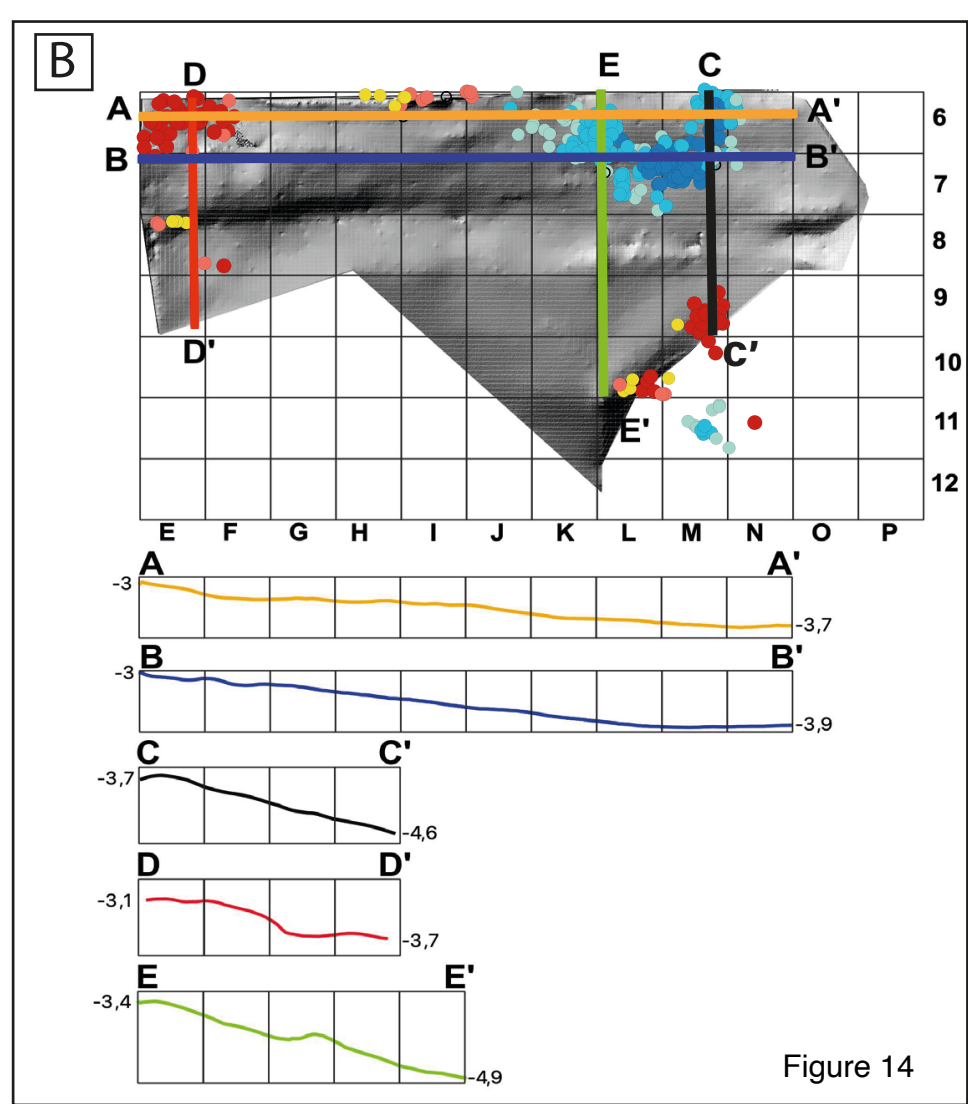
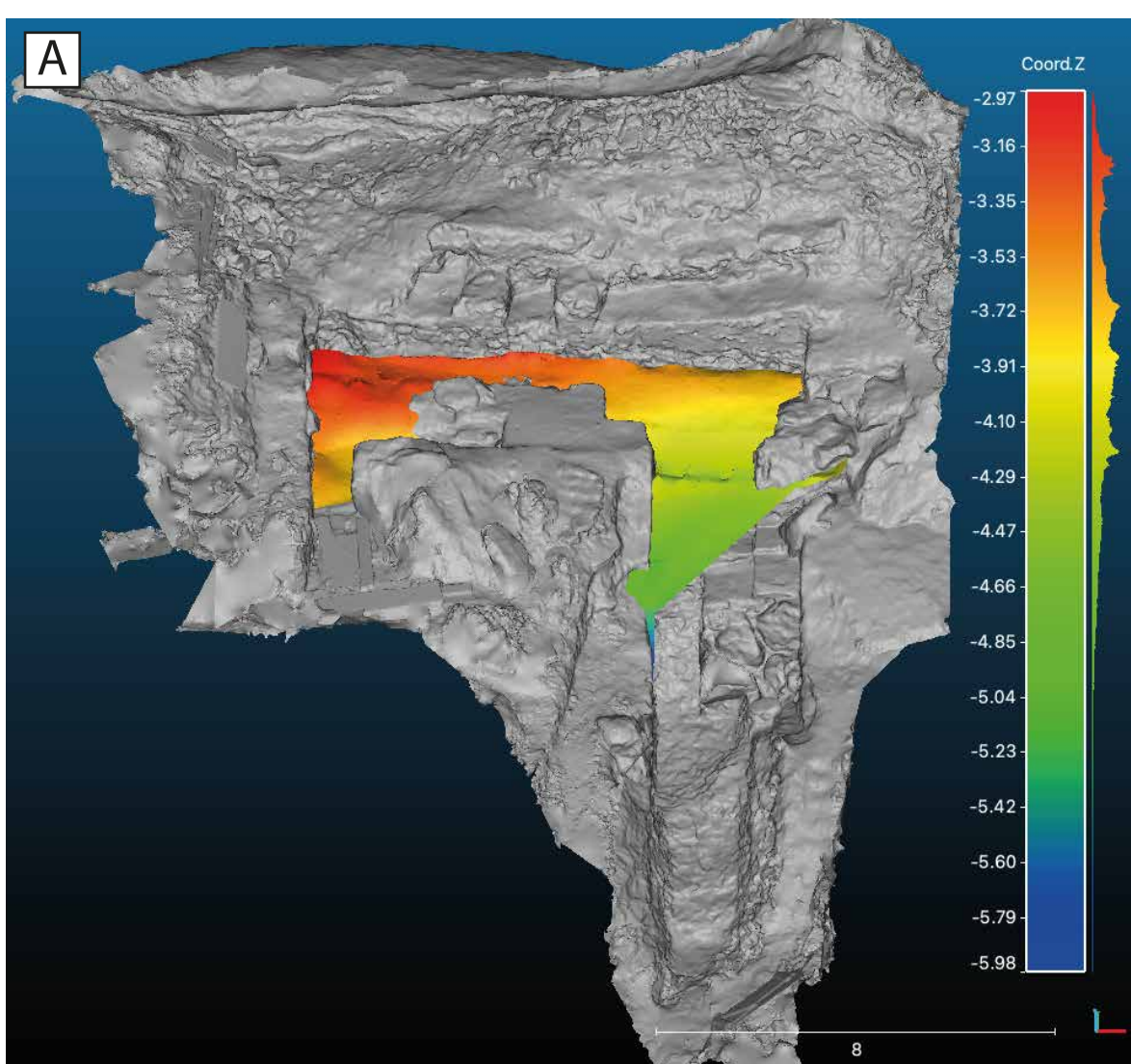
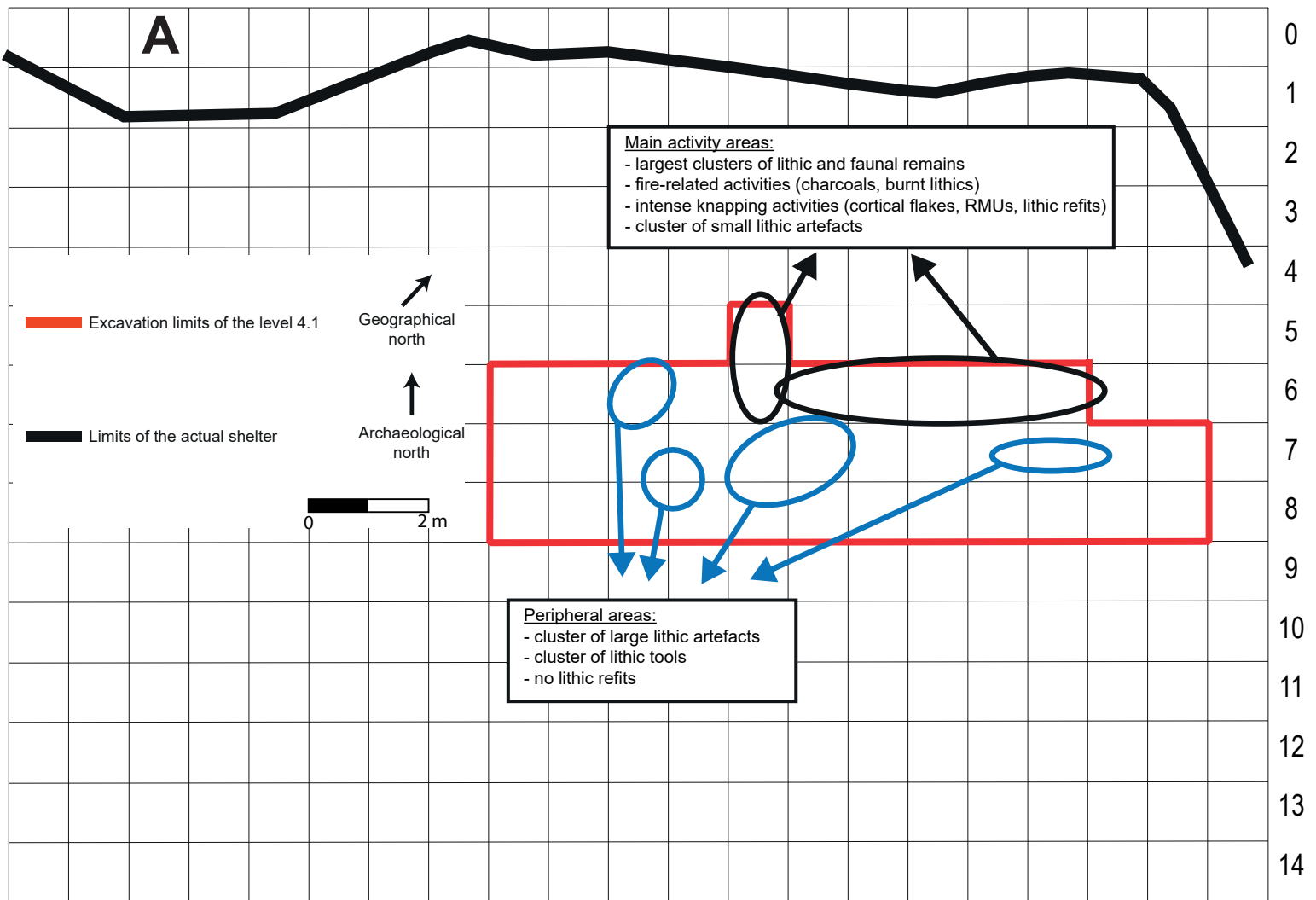


Figure 14

Figure 15

A B C D E F G H I J K L M N O P Q



A B C D E F G H I J K L M N O P Q

